In addition, recent studies have revealed that aberrations in FXR are involved in liver carcinogenesis. FXR deficiency in mice leads to the development of neoplasms in the liver, including hepatic adenoma, HCC, and hepatocholangiocellular carcinoma [15,16]. A significant decrease in FXR expression and activity is also observed in human HCC samples [17]. Therefore, targeting FXR and improving its function might be a promising strategy for the prevention and treatment of HCC.

Recently, combination therapy and prevention have garnered much interest in the cancer field because they can synergistically inhibit growth and induce apoptosis in cancer cells. In human HCC-derived cells, ACR acts synergistically with other agents, such as interferon (IFN)-β, OSI-461, vitamin K_2, valproic acid, and trastuzumab, in suppressing growth and inducing apoptosis [11,18–21]. The agents that inhibit RXRα phosphorylation are among the most promising agents to use in combination with ACR [11,20,21]. In addition, the induction of nuclear receptors that dimerize with RXR, such as retinoic acid receptor (RAR)-β, and activation of these receptors by their ligands may also lead to synergistic growth inhibition in HCC cells when combined with ACR [11,19]. GW4064, a synthetic ligand for FXR, is known to induce the expression of genes involved in the transport of bile acids in the liver and intestines [22,23]. GW4064 also inhibits the growth of breast and prostate cancer cell lines [24–26], whereas the anticancer effects of this agent on HCC cells have not been evaluated. In the present study, we examined the effects of GW4064 on the growth of human HCC cells. We also investigated whether the combination of ACR plus GW4064 exerts synergistic growth inhibitory effects on HCC cells and examined the possible mechanisms responsible for such synergy.

2. Materials and methods

2.1. Materials

ACR (NIK-333) was supplied by Kowa Pharmaceutical Co. Ltd., (Tokyo, Japan). GW4064 was purchased from Sigma–Aldrich (St. Louis, MO, USA). The anti-RXRα antibody was from Santa Cruz Biotechnology (Santa Cruz, CA, USA). The primary antibodies for ERK, phosphorylated ERK (p-ERK), Stat3, phosphorylated Stat3 (p-Stat3), PARP, and GAPDH were from Cell Signaling Technology (Beverly, MA, USA).

2.2. Cell lines and cell culture conditions

HLE, HLF, and Huh7 human HCC cell lines were obtained from the Japanese Cancer Research Resources Bank (Tokyo, Japan). HLE and HLF cells were maintained in DMEM and Huh7 cells were in RPMI1640 media, respectively. All media were supplemented with 10% FCS and 1% Penicillin/Streptomycin. Hc human normal hepatocyte cell line was purchased from Cell Systems (Kirkland, WA, USA) and maintained in a CS-S complete medium (Cell Systems). These cells were cultured in an incubator with humidified air with 5% CO_2 at 37 °C.

2.3. Cell proliferation assays

One thousand of HCC (HLE, HLF, and Huh7) or Hc cells were seeded on 96-well plates. The following day, the medium was changed to serum free medium and the cells were treated with the indicated concentrations of ACR or GW4064 for 48 h. Cell proliferation assays were performed using a MTS assay (Promega, Madison, WI, USA) according to the manufacturer's instructions. To determine whether the combined effects of ACR plus GW4064 were synergistic, HCC cells were treated with combinations of the indicated concentrations of ACR and GW4064 for 48 h and the combination index (CI)-isobologram was calculated. Variable ratios of drug concentrations were used in the studies, and mutually exclusive equations were used to determine the CIs. Each CI was calculated from the mean affected fraction at each drug ratio concentration (triplicate), as described previously [11,19,27].

2.4. Apoptosis assays

TUNEL, caspase-3 activity, and Annexin V assays are conducted to evaluate apoptosis. For TUNEL assay, HLE cells (1×10^6) were treated with 1 μM ACR alone, 1 μM GW4064 alone, or the combination of these agents for 48 h on glass bottom culture dishes. The cells were then fixed with 4% paraformaldehyde at room temperature for 10 min, permeabilized with 0.3% Triton X-100 in TBS (pH 7.4), and stained with both 4',6-diamidino-2-phenylindole (DAPI) and terminal deoxynucleotidyl transferase-mediated dUTP nick-end labeling (TUNEL) methods using the *In Situ* Cell Death Detection Kit, Fluorescein (Roche Diagnostics, Mannheim, Germany) [11].

Caspase-3 activity and Annexin V assays were performed using HLE cells that were treated with the same concentration of test drugs for 72 h. The cell lysates were prepared and the caspase-3 activity assay was done using the Apoalert Caspase Fluorescent Assay Kit (Clontech Laboratories, Mountain View, CA, USA). The Annexin V-binding capacity of treated cells was investigated by flow cytometry using the Annexin V-FITC apoptosis detection kit I (BD, Franklin Lakes, NJ, USA). Cultured cells were washed with cold phosphate-buffered saline before incubation with Annexin V-FITC in a buffer containing propidium iodine (PI). Stained cells were analyzed by flow cytometry using the FACScan (BD). Annexin V-FITC-positive and PI negative cells were considered to be populations undergoing apoptosis.

2.5. Cell cycle assays

HLE cells were treated with 1 μM ACR alone, 1 μM GW4064 alone, or the combination of these agents for 72 h in DMEM medium with 1% FCS. The harvested cells were stained with PI using Cell Cycle Phase Determination Kit (Cayman, Ann Arbor, MI, USA), and the samples were then analyzed for DNA histograms and cell cycle phase distribution using a FACScan flow cytometer. The data were analyzed by using the CellQuest computer program (BD) [11].

2.6. Protein extraction and Western blot analysis

Equivalent amounts of extracted protein were examined by a Western blot analysis using specific antibodies [21]. To detect the expression level of phosphorylated RXRα (p-RXRα) protein, total phosphoprotein was affinity-purified from the total cell extracts using a PhosphoProtein Purification Column (QIAGEN, Valencia, CA, USA) and then was subjected to the Western blot analyses using an anti-RXRα antibody. GAPDH expression served as a loading control. The intensities of protein bands were quantified using NIH image software version 1.45.

2.7. RNA extraction and quantitative RT-PCR analysis

Total RNA was isolated from the HLE cells using the RNAqueous-4PCR kit (Ambion Applied Biosystems, Austin, TX, USA) and cDNA was amplified from 0.2 μg of total RNA using the SuperScript III First-Strand Synthesis System (Invitrogen, Carlsbad, CA, USA) [28]. Quantitative real-time reverse transcription-PCR (RT-PCR) analysis was performed using specific primers that amplify the *c-myc*, small heterodimer partner (SHP), $p21^{CIP1}$, cyclin D1, and β-actin genes. The specific primer sets for $p21^{CIP1}$, cyclin D1, and β-actin were used as described elsewhere [12,29]. The sequences for *c-myc*- and SHP-specific primers were as follows: FMYC (5'-CCC TGA GCG ATT CAG ATG AT-3') and RMYC (5'-GCT CCA GGA TGT TGT GGT TT-3'), and FSHP (5'-GCT GTC TGG AGT CCT TCT GG-3') and RSHP (5'-ACC TGA GCA AAA GCA TGT CC-3'), respectively.

2.8. FXRE reporter assays

HLE cells were transfected with FXR response element (FXRE) reporter plasmids (100 ng/well in 96-well dish), which were kindly provided by Dr. T. Nishimaki-Mogami (National Institute of Health Sciences, Tokyo, Japan), along with p*RL*-CMV (*Renilla* luciferase, 10 ng/well in 96-well dish; Promega) as an internal standard to normalize the transfection efficiency. Transfections were done using Lipofectamine LTX Reagent (Invitrogen). After exposure of the cells to the transfection mixture for 24 h, the cells were treated with 1 μM ACR alone, 1 μM GW4064 alone, or the combination of these agents for 24 h. The cell lysates were then prepared, and the luciferase activity of each cell lysate was determined using a dual-luciferase reporter assay system (Promega) [11].

2.9. Statistical analysis

The data are expressed as the means ± SD. Statistical significance of the differences in the mean values was assessed with a one-way ANOVA, followed by Tukey–Kramer's multiple comparison tests. Values of $P < 0.05$ were considered to be significant.

3. Results

3.1. ACR and GW4064 cause preferential inhibition of the growth of human HCC cells in comparison with Hc normal hepatocytes

In our initial study, we examined the growth inhibitory effect of ACR and GW4064 on HLE, HLF, and Huh7 human HCC cells and on Hc hepatocytes. ACR inhibited the growth of HCC cells with an IC_{50} value of less than 4 μM. The HLF cells were most susceptible to ACR

because the IC_{50} value with this agent was 2 μM (Fig. 1A). GW4064 also inhibited the growth of this series of HCC cells with an IC_{50} value of about 1.4 μM (Fig. 1B). On the other hand, Hc cells were resistant to these agents up to 5 μM (Fig. 1). These results suggest that ACR and GW4064 preferentially inhibit the growth of HCC cells compared with that of normal hepatocytes.

3.2. ACR plus GW4064 cause synergistic inhibition of the growth of HCC cells

Next, the effects of combined treatment were examined with a range of concentrations of ACR plus GW4064 to determine whether they synergistically inhibited the growth of HLE (Fig. 2A), HLF (Fig. 2B), and Huh7 (Fig. 2C) HCC cells. We found that the CI indices for less than 1 μM ACR (0.5 or 1 μM) plus less than 0.5 μM GW4064 (0.1 or 0.5 μM) were 1+(slight synergism), 2+(moderate synergism), or 3+(synergism), respectively, in this series of HCC cells (Fig. 2D and Table 1). These findings suggest that ACR plus GW4064 might be an effective combination for the inhibition of HCC cell growth due to their synergistic activity. The combination of 1 μM ACR (about IC_{25} value) and 1 μM GW4064 (about IC_{30} value) in HLE cells (Fig. 2A and D, and Table 1) was used for the following experiments because a CI-isobologram analysis gave this combination a CI index of 1+(0.88), indicating slight synergism.

3.3. ACR plus GW4064 cooperatively induce apoptosis in HLE cells

We next examined whether the synergistic growth inhibition in HLE cells induced by treatment with ACR plus GW4064 might be associated with the induction of apoptosis. In TUNEL assays, the treatment of HLE cells with either 1 μM ACR or 1 μM GW4064 alone induced TUNEL-positive cells in approximately 19.3% or 11.9% of the total viable cells, respectively. However, the combination of these agents markedly enhanced the induction of apoptosis, with 51.6% of the total viable cells being TUNEL-positive (Fig. 3A). Similar results were also observed in the Western blot analysis for PARP expression; the combination of ACR plus GW4064 markedly enhanced PARP cleavage, indicating the induction of apoptosis (Fig. 3B). We also found an increase in the levels of caspase-3 activity in ACR alone- and GW4064 alone-treated cells, and this was significantly enhanced when the cells were treated with a combination of these agents (Fig. 3C). In addition, the percentage of Annexin V-positive cells, which was increased by treatment with GW4064 alone, was substantially increased by the combined treatment with ACR plus GW4064 (Fig. 3D). These findings suggest that the combination with ACR plus GW4064 synergistically inhibited growth of HLE human HCC cells, mainly, through the induction of apoptosis.

3.4. ACR plus GW4064 cooperatively induce G_0/G_1 cell cycle arrest in HLE cells

A cell cycle analysis was performed using DNA flow cytometry to determine whether the synergistic effects on growth inhibition caused by combined treatment with ACR plus GW4064 were associated with specific changes in cell cycle distribution. As shown in Fig. 4, the combined treatment with 1 μM ACR plus 1 μM GW4064 significantly increased the percentage of cells in the G_0/G_1 phase in comparison to that of untreated cells (76.1 ± 4.3% vs. 57.3 ± 5.8%, $P < 0.05$), whereas the population of cells in this phase was not significantly increased by treatment with ACR alone (63.6 ± 3.0%) or GW4064 alone (65.3 ± 4.5%). These findings suggest that the combination of ACR plus GW4064 cooperatively induced G_0/G_1 phase cell cycle arrest in HLE human HCC cells.

3.5. ACR plus GW4064 additively suppress the phosphorylation of RXRα, ERK, and Stat3 proteins in HLE cells

RXRα phosphorylation plays a critical role in the development of HCC and might be a promising target for HCC chemoprevention [4–8]. Therefore, the effects of the combination of ACR plus GW4064 on the phosphorylation of this nuclear receptor and related signaling molecules were investigated in HLE cells. As shown in Fig. 5, when the cells were treated with 1 μM ACR, there was a marked decrease in the expression levels of p-RXRα and p-Stat3 proteins. Treatment with 1 μM GW4064 alone also decreased the expression levels of p-ERK and p-Stat3 protein. Moreover, the expression levels of p-RXRα, p-ERK and p-Stat3 proteins were markedly decreased when the cells were treated with the combination of these agents.

3.6. ACR plus GW4064 cooperatively affect the expression levels of $p21^{CIP1}$, c-myc, cyclin D1, and SHP mRNA in HLE cells

We next examined the combined effects of ACR plus GW4064 on the expression levels of $p21^{CIP1}$, c-*myc*, and cyclin D1 mRNA in HLE cells because these genes control cell proliferation and cell cycle progression. The quantitative RT-PCR analyses revealed that treatment with neither 1 μM ACR nor 1 μM GW4064 alone had any apparent effect on the expression levels of $p21^{CIP1}$, c-*myc*, and cyclin D1 mRNA. However, when the cells were treated with the combination of these agents, there was a significant increase

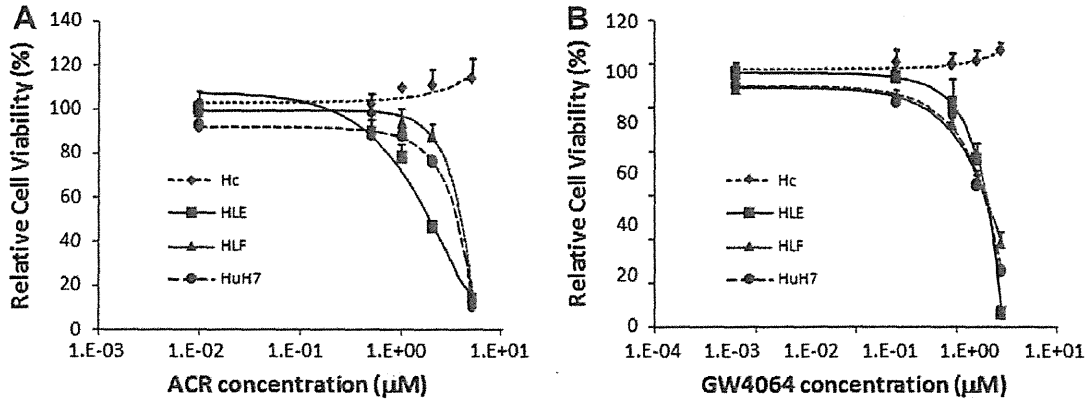

Fig. 1. Inhibition of cell growth by ACR and GW4064 in HLE, HLF, and Huh7 human HCC cells and Hc normal hepatocytes. HLE, HLF, Huh7, and Hc cells were treated with the indicated concentrations of ACR (A) or GW4064 (B) for 48 h. Cell viability was determined by MTS assay and was expressed as a percentage of the control value. *Error Bars*, SD of triplicate assays.

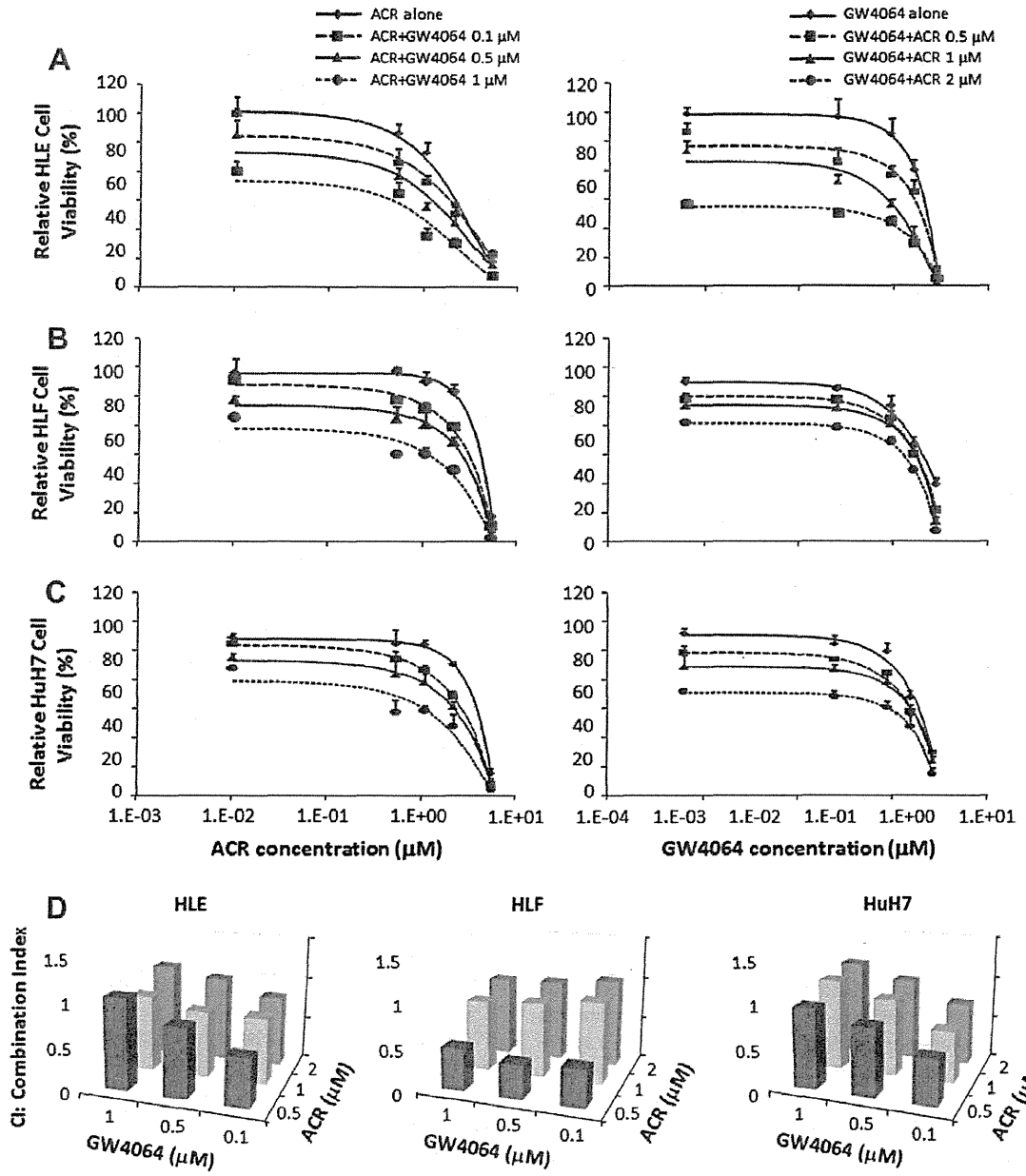

Fig. 2. Inhibition of cell growth by ACR alone, GW4064 alone, and various combinations of these agents in HCC cells. HLE (A), HLF (B), and Huh7 (C) cells were treated with the indicated concentrations of ACR alone, GW4064 alone, and various combinations of these agents for 48 h. Cell viability was determined by MTS assay and expressed as a percentage of the control value. *Error Bars*, SD of triplicate assays. (D) The data obtained in (A), (B), and (C) was used to calculate the combination index.

Table 1
Combined effects of ACR and GW4064 on HCC cells.

	HLE ACR concentration (μM)			HLF ACR concentration (μM)			HuH7 ACR concentration (μM)		
GW4064 concentration (μM)	0.5	1	2	0.5	1	2	0.5	1	2
0.1	+++	++	+	+++	+	±	+++	++	++
0.5	++	++	±	+++	++	±	++	+	±
1	±	+	±	+++	+	±	±	±	±

Note: "±", CI 0.9–1.1 additive effect; " + ", CI 0.8–0.9 slight synergism; "++", CI 0.6–0.8 moderate synergism; "+++", CI 0.4–0.6 synergism;
Abbreviations: CI, combination index; ACR, acyclic retinoid.

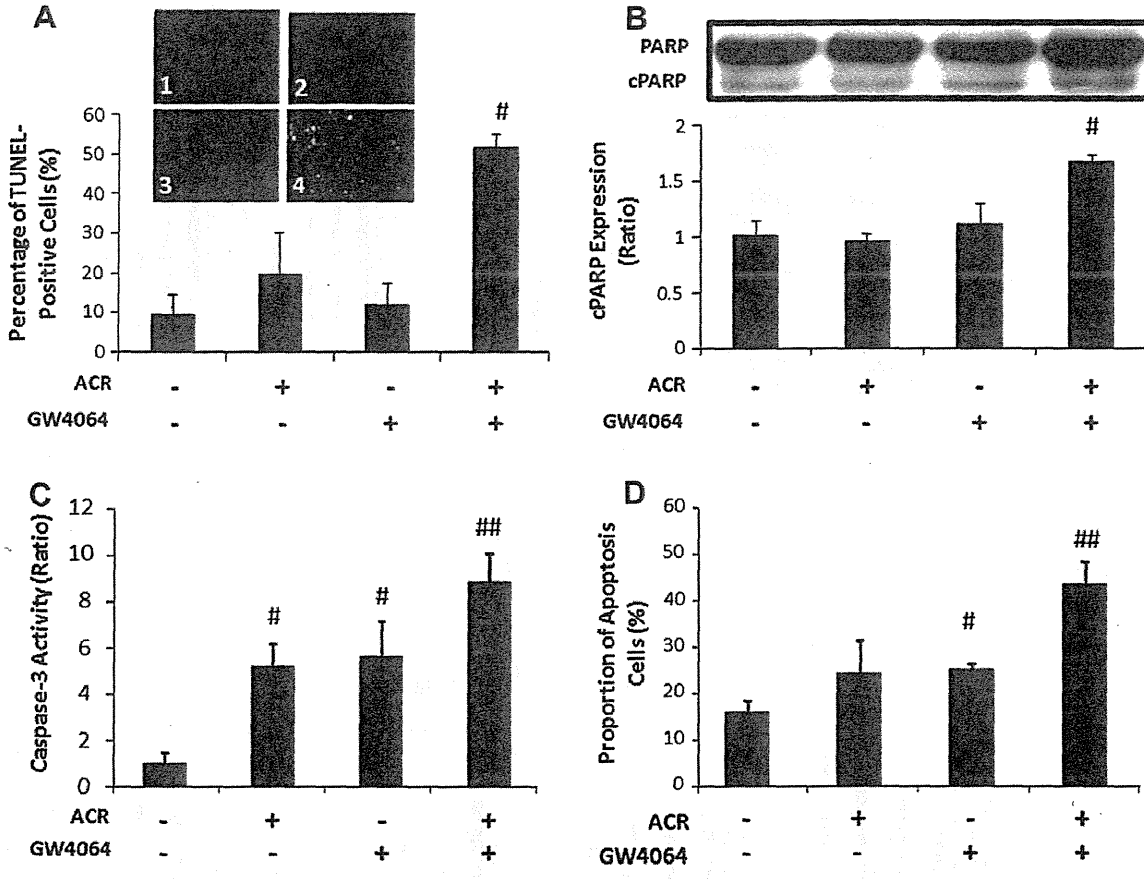

Fig. 3. Effects of the combination of ACR plus GW4064 on induction of apoptosis in HLE cells. The cells were treated with vehicle, 1 μM ACR alone, 1 μM GW4064 alone, or the combination of 1 μM ACR plus 1 μM GW4064 for 48 h or 72 h. TUNEL assays (A) and Western blot analysis using a PARP-specific antibody (B, upper panel) were performed using cells treated with test drugs for 48 h. Caspase-3 activity assays (C) and Annexin V assays (D) were performed using samples treated for 72 h. (A) TUNEL-positive cells were counted and examined as the percentage of the DAPI-positive cell number (500 cells were counted in each flask). (B) The intensities of the cleaved PARP (c-PARP) blots were quantified using densitometry. Columns and lines indicate mean and SD of triplicate assays (lower panel). (C) Caspase-3 activity was performed with a fluorometric system. (D) Cultured cells were incubated with Annexin V-FITC in a buffer containing propidium iodine (PI). Stained cells were then analyzed by flow cytometry. Annexin V-FITC-positive and PI-negative cells were counted as apoptotic cells. #: $P < 0.05$, compared with vehicle treated cells. ##: $P < 0.05$, compared with vehicle, ACR alone, or GW4064 alone treated cells.

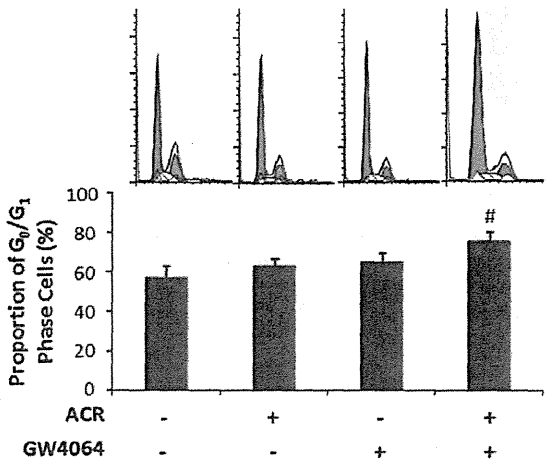

Fig. 4. Effects of the combination of ACR plus GW4064 on induction of the G_0/G_1 cell cycle arrest in HLE cells. HLE cells were treated with vehicle, 1 μM ACR alone, 1 μM GW4064 alone, or the combination of 1 μM ACR plus 1 μM GW4064 for 72 h. The cells were then stained with propidium iodide to analyze their cell cycle progression. The distributions of cells in the G_0/G_1 of the cell cycle were calculated using a FACScan. *Error Bars*, SE of triplicate assays. #: $P < 0.05$, compared with vehicle treated cells.

in the levels $p21^{CIP1}$, and a decrease in the levels of c-*myc* and cyclin D1 mRNA expression (Fig. 6A–C). In addition, the expression level of SHP mRNA, which is one of the target genes of FXR [17,25,30,31], was also significantly increased by the combination treatment with ACR plus GW4064 (Fig. 6D).

3.7. ACR enhances the induction of FXRE promoter activities by GW4064

FXR and RXRs modulate the expression of target genes by interacting with FXRE elements located in the promoter regions of such genes [13]. Therefore, we next examined whether ACR might enhance the transcriptional activity of the FXRE promoter induced by GW4064 using transient transfection luciferase reporter assays. As shown in Fig. 6E, 1 μM GW4064 significantly increased the FXRE reporter activity in comparison with control HLE cells which were not treated with either ACR or GW4064. Moreover, when the cells were treated with a combination of 1 μM GW4064 plus 1 μM ACR, there was a significant increase in the transcriptional activity of the FXRE reporter, thus suggesting that treatment with these agents might cooperatively enhance the FXRE reporter activity.

4. Discussion

The prognosis for patients with HCC is poor and more effective strategies for the chemoprevention and chemotherapy of this malignancy are urgently required. The present study provides the

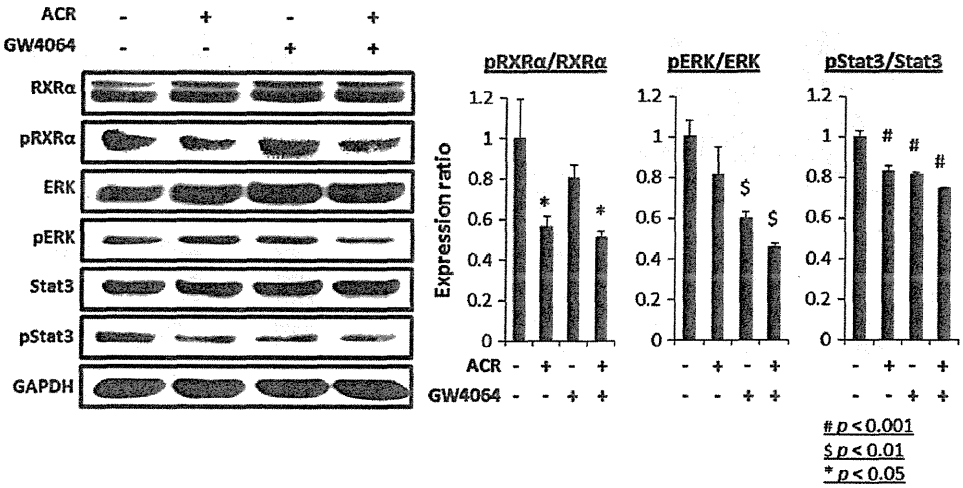

Fig. 5. Effects of the combination of ACR plus GW4064 on the phosphorylation of RXRα, ERK, and Stat3 proteins in HLE cells. HLE cells were treated with vehicle, 1 μM ACR alone, 1 μM GW4064 alone, or the combination of 1 μM ACR plus 1 μM GW4064 for 12 h. The extracted proteins were examined by a Western blot analysis using the respective antibodies (left panels). The intensities of the blots were quantified using densitometry. Columns and lines indicate means and SD of triplicate assays (right panels). Repeat Western blots gave similar results. □: $P < 0.05$, $: $P < 0.01$, #: $P < 0.001$, compared with vehicle treated cells.

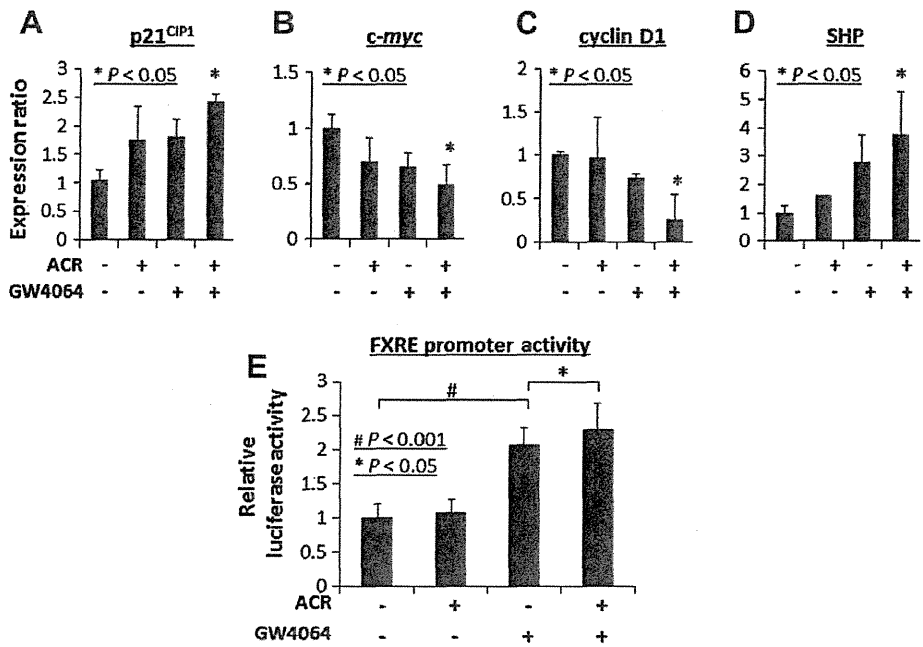

Fig. 6. Effects of the combination of ACR plus GW4064 on the expression of $p21^{CIP1}$, *c-myc*, cyclin D1, and SHP mRNA and on the transcriptional activity of the FXRE promoter in HLE cells. HLE cells were treated with vehicle, 1 μM ACR alone, 1 μM GW4064 alone, or the combination of 1 μM ACR plus 1 μM GW4064 for 24 h. The extracted mRNAs were examined by a quantitative real-time RT-PCR analysis using the $p21^{CIP1}$ (A), *c-myc* (B), cyclin D1 (C), and SHP (D) specific primers. The expression levels of each mRNA were normalized to the level of β-actin mRNA. Values represent the means ± SD of triplicate analyses. *: $P < 0.05$. (E) A transient transfection reporter assay was performed with the FXRE luciferase reporter in the presence of vehicle, 1 μM ACR alone, 1 μM GW4064 alone, or the combination of 1 μM ACR plus 1 μM GW4064. Relative luciferase activity was determined after 24 h. Columns and lines indicate the means and SD of triplicate assays. #: $P < 0.001$, **: $P < 0.05$.

first evidence that GW4064, a synthetic ligand for FXR, preferentially inhibits the growth of HCC cells compared with Hc normal hepatocytes. This study also clearly indicates that the combination of GW4064 plus ACR, which is expected as a HCC chemopreventive agent [8–10], cause a synergistic inhibition of growth in HLE human HCC cells and that this is associated with the induction of apoptosis. This combination also acted cooperatively to induce the arrest of the cell cycle in the G_0/G_1 phase and the expression of $p21^{CIP1}$ and SHP mRNA, but suppress the expression levels of *c-myc* and cyclin D1 mRNA.

As illustrated in Fig. 7, we presume that the synergism generated by the combination of ACR plus GW4064 is mainly associated with the enhancement of the FXRE reporter activity. FXR regulates the expression of target genes by binding either as a monomer or as a heterodimer with RXR to the FXRE [13]. Therefore, in the present study, ACR and GW4064 cooperatively enhanced the binding of FXR to the FXRE promoter, thereby enhancing the expression of its target genes (Fig. 7, as indicated by A). Among the FXR target genes, SHP is considered to play a role in the inhibition of cell growth because it is a pivotal cell death receptor that targets the mitochondria, leading to the induction of apoptosis and inhibition of tumor growth [32]. GW4064 suppresses the growth of cancer cells through the activation of FXR targeted genes, including SHP [17,25,30,31]. SHP has also been shown to be a direct negative

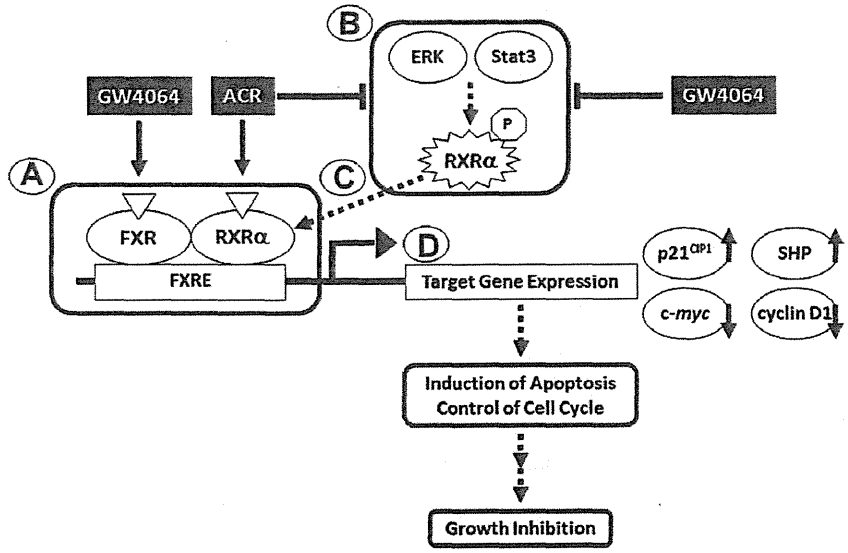

Fig. 7. A hypothetical schematic representation of the effects of the combination of ACR plus GW4064 on growth inhibition in HCC cells. ACR and GW4064 can bind to their receptors, RXRα and FXR, as ligands, and subsequently activate the FXRE promoter activity (A). ACR and GW4064 also inhibit RXRα phosphorylation, which is involved in liver carcinogenesis, by inhibiting ERK and Stat3 phosphorylation (B). The inhibition of RXRα phosphorylation by these agents might restore the function of this nuclear receptor as a heterodimeric partner for FXR (C), thus resulting in the activation of the FXRE promoter activity. Cooperative activation of this promoter activity by ACR and GW4064 regulates the expression of target genes, such as $p21^{CIP1}$, *c-myc*, cyclin D1, and SHP, which play a critical role in the induction of apoptosis, control of cell cycle progression, and inhibition of cancer cell growth (D). For additional details see Section 4.

regulator of cyclin D1 gene transcription [30]. Treatment with 1 μM GW4064 alone did not significantly increase the expression levels of SHP mRNA in the present study, whereas its expression was clearly increased by combined treatment with ACR plus GW4064. These findings may indicate that the concentration of 1 μM is insufficient to increase the levels of SHP mRNA in HCC cells and, therefore, an appropriate partner, such as ACR, is required for GW4064 to exert a synergistic effect on growth inhibition in HCC cells (Fig. 7).

In addition, recent studies have revealed that activating FXR suppresses the expression of cyclin D1 and c-*myc*, but induces the expression of $p21^{CIP1}$, by targeting the Wnt/β-catenin signaling pathway [17,31]. These findings seem to be significant because the Wnt/β-catenin pathway plays a critical role in liver carcinogenesis, and thus may be a promising target for the treatment of HCC [33]. In FXR knockout mice, sustained activation of this pathway was shown to be involved in the development of HCC [17]. On the other hand, ACR has been shown to exert growth inhibitory effects in HCC cells by targeting the Wnt/β-catenin pathway [12]. ACR also induces apoptosis and cell cycle arrest in the G_0/G_1 phase in HCC cells by regulating the expression of $p21^{CIP1}$, cyclin D1, and c-*myc* [12,19,34,35]. Therefore, the activation of FXR by GW4064 may act cooperatively with ACR to inhibit the activation of the Wnt/β-catenin pathway, subsequently decreasing the expression of cyclin D1 and c-*myc*, but increasing the expression of $p21^{CIP1}$, as was demonstrated in the present study.

In addition to chronic inflammation and subsequent cirrhosis of the liver induced by persistent infection with hepatitis virus, increased evidence has indicated that a malfunction of RXRα due to phosphorylation is profoundly involved in the development of HCC [4–8]. In HCC cells, the Ras/MAPK signaling pathway is highly activated, leading to phosphorylation of RXRα, which indicates that the Ras/MAPK pathway and p-RXRα are potential targets for inhibiting the growth of HCC cells [4–8]. Indeed, ACR dephosphorylates RXRα, ERK, and Stat3 proteins, and restores the function of RXRα, thus inhibiting the growth of HCC cells and suppressing liver tumorigenesis in obese mice [4,11,20,36]. The combinations of ACR plus valproic acid or vitamin K_2 also synergistically suppressed the growth of HCC cells by inhibiting RXRα phosphorylation [11,20]. Similar to these previous studies [11,20], in the present study, inhibition of RXRα phosphorylation by the combination of ACR plus GW4064 may also have restored the function of RXRα as a master regulator of nuclear receptors, thus contributing to synergistic growth inhibition in HCC cells (Fig. 7, as indicated by B). Dephosphorylation of RXRα by this combination treatment may play a role in the observed enhancement of the FXRE promoter activity because phosphorylation of RXRα abolishes its ability to form heterodimers with other nuclear receptors, but inhibition of this phosphorylation can restore its heterodimeric activity [7]. The combination of ACR plus GW4064 may also promote RXRs homodimerization and thus enhance the promoter activity of retinoid X response element, which is associated with the anticancer mechanisms of ACR [11,37].

One of the major questions that arose was how the combination of ACR plus GW4064 could inhibit the phosphorylation of ERK and Stat3 proteins. One of the mechanisms which might explain this phenomenon is that the effects of ACR and GW4064 inhibit the activation of specific receptor tyrosine kinases (RTKs). ACR has been shown to reduce HCC development and inhibit cancer growth by targeting growth factors and their corresponding RTKs, such as the epidermal growth factor (EGF) receptor (EGFR), and downstream signaling pathways, including the Ras/MAPK and Jak/Stat3 pathways [29,38]. The activation of FXR by its ligand also reduces the expression of HER2, a member of the EGFR family of RTKs, and inhibits EGF-mediated HER2 and ERK phosphorylation in human breast cancer cells [24]. Therefore, GW4064 may increase the inhibitory effects of ACR on certain types of RTKs by activating FXR, which results in the inhibition of ERK and Stat3 phosphorylation and subsequent RXRα phosphorylation. Future studies are required to clarify whether both ACR and GW4064 synergistically exert inhibitory effects on the activation of specific RTKs.

Finally, it should be noted that, in a clinical trial showing the chemopreventive effects of ACR on the recurrence of secondary HCC [9,10], the plasma concentration of this agent (which ranged from 1 to 5 μM) was approximately the same as the concentration used in the present study (1 μM). In phase II clinical trials, a FXR

ligand also ameliorated the increase in the alkaline phosphatase levels in patients with primary biliary cirrhosis and improved the insulin sensitivity in patients with diabetes and liver steatosis, although some unfavorable events that might be associated with FXRE reporter overactivity were observed [39]. The combination of ACR plus GW4064 may resolve such problems because this combination permits the administration of lower doses of both agents for treatment. Future pharmacokinetic studies are required to determine whether the dose of GW4064 used in this study is clinically relevant and pilot studies confirming are thus called for to clarify the safety of this agent.

In conclusion, the observation that a combination of appropriate concentrations of ACR plus GW4064 can inhibit the growth of human HCC cells without affecting the growth of normal hepatocytes should encourage further clinical studies using these agents to investigate their potential for HCC chemoprevention and chemotherapy. The results of our present study suggest that combining ACR with GW4064 might hold promise as a clinical modality for the prevention and treatment of HCC, due to their synergistic effects.

References

[1] D.J. Mangelsdorf, C. Thummel, M. Beato, P. Herrlich, G. Schutz, K. Umesono, B. Blumberg, P. Kastner, M. Mark, P. Chambon, R.M. Evans, The nuclear receptor superfamily: the second decade, Cell 83 (1995) 835–839.

[2] P. Chambon, A decade of molecular biology of retinoic acid receptors, Faseb. J. 10 (1996) 940–954.

[3] L. Altucci, M.D. Leibowitz, K.M. Ogilvie, A.R. de Lera, H. Gronemeyer, RAR and RXR modulation in cancer and metabolic disease, Nat. Rev. Drug Discov. 6 (2007) 793–810.

[4] R. Matsushima-Nishiwaki, M. Okuno, Y. Takano, S. Kojima, S.L. Friedman, H. Moriwaki, Molecular mechanism for growth suppression of human hepatocellular carcinoma cells by acyclic retinoid, Carcinogenesis 24 (2003) 1353–1359.

[5] R. Matsushima-Nishiwaki, M. Okuno, S. Adachi, T. Sano, K. Akita, H. Moriwaki, S.L. Friedman, S. Kojima, Phosphorylation of retinoid X receptor alpha at serine 260 impairs its metabolism and function in human hepatocellular carcinoma, Cancer Res. 61 (2001) 7675–7682.

[6] S. Adachi, M. Okuno, R. Matsushima-Nishiwaki, Y. Takano, S. Kojima, S.L. Friedman, H. Moriwaki, Y. Okano, Phosphorylation of retinoid X receptor suppresses its ubiquitination in human hepatocellular carcinoma, Hepatology 35 (2002) 332–340.

[7] K. Yoshimura, Y. Muto, M. Shimizu, R. Matsushima-Nishiwaki, M. Okuno, Y. Takano, H. Tsurumi, S. Kojima, Y. Okano, H. Moriwaki, Phosphorylated retinoid X receptor alpha loses its heterodimeric activity with retinoic acid receptor beta, Cancer Sci. 98 (2007) 1868–1874.

[8] M. Shimizu, K. Takai, H. Moriwaki, Strategy and mechanism for the prevention of hepatocellular carcinoma: phosphorylated retinoid X receptor alpha is a critical target for hepatocellular carcinoma chemoprevention, Cancer Sci. 100 (2009) 369–374.

[9] Y. Muto, H. Moriwaki, M. Ninomiya, S. Adachi, A. Saito, K.T. Takasaki, T. Tanaka, K. Tsurumi, M. Okuno, E. Tomita, T. Nakamura, T. Kojima, Prevention of second primary tumors by an acyclic retinoid, polyprenoic acid, in patients with hepatocellular carcinoma. Hepatoma prevention study group, New Engl. J. Med. 334 (1996) 1561–1567.

[10] Y. Muto, H. Moriwaki, A. Saito, Prevention of second primary tumors by an acyclic retinoid in patients with hepatocellular carcinoma, New Engl. J. Med. 340 (1999) 1046–1047.

[11] H. Tatebe, M. Shimizu, Y. Shirakami, H. Sakai, Y. Yasuda, H. Tsurumi, H. Moriwaki, Acyclic retinoid synergises with valproic acid to inhibit growth in human hepatocellular carcinoma cells, Cancer Lett. 285 (2009) 210–217.

[12] M. Suzui, M. Masuda, J.T. Lim, C. Albanese, R.G. Pestell, I.B. Weinstein, Growth inhibition of human hepatoma cells by acyclic retinoid is associated with induction of p21(CIP1) and inhibition of expression of cyclin D1, Cancer Res. 62 (2002) 3997–4006.

[13] Y.D. Wang, W.D. Chen, D.D. Moore, W. Huang, FXR: a metabolic regulator and cell protector, Cell Res. 18 (2008) 1087–1095.

[14] W. Huang, K. Ma, J. Zhang, M. Qatanani, J. Cuvillier, J. Liu, B. Dong, X. Huang, D.D. Moore, Nuclear receptor-dependent bile acid signaling is required for normal liver regeneration, Science 312 (2006) 233–236.

[15] F. Yang, X. Huang, T. Yi, Y. Yen, D.D. Moore, W. Huang, Spontaneous development of liver tumors in the absence of the bile acid receptor farnesoid X receptor, Cancer Res. 67 (2007) 863–867.

[16] I. Kim, K. Morimura, Y. Shah, Q. Yang, J.M. Ward, F.J. Gonzalez, Spontaneous hepatocarcinogenesis in farnesoid X receptor-null mice, Carcinogenesis 28 (2007) 940–946.

[17] A. Wolfe, A. Thomas, G. Edwards, R. Jaseja, G.L. Guo, U. Apte, Increased activation of the Wnt/{beta}-catenin pathway in spontaneous hepatocellular carcinoma observed in farnesoid x receptor knockout mice, J. Pharmacol. Exp. Ther. 338 (2011) 12–21.

[18] A. Obora, Y. Shiratori, M. Okuno, S. Adachi, Y. Takano, R. Matsushima-Nishiwaki, I. Yasuda, Y. Yamada, K. Akita, T. Sano, J. Shimada, S. Kojima, Y. Okano, S.L. Friedman, H. Moriwaki, Synergistic induction of apoptosis by acyclic retinoid and interferon-beta in human hepatocellular carcinoma cells, Hepatology 36 (2002) 1115–1124.

[19] M. Shimizu, M. Suzui, A. Deguchi, J.T. Lim, D. Xiao, J.H. Hayes, K.P. Papadopoulos, I.B. Weinstein, Synergistic effects of acyclic retinoid and OSI-461 on growth inhibition and gene expression in human hepatoma cells, Clin. Cancer Res. 10 (2004) 6710–6721.

[20] T. Kanamori, M. Shimizu, M. Okuno, R. Matsushima-Nishiwaki, H. Tsurumi, S. Kojima, H. Moriwaki, Synergistic growth inhibition by acyclic retinoid and vitamin K_2 in human hepatocellular carcinoma cells, Cancer Sci. 98 (2007) 431–437.

[21] H. Tatebe, M. Shimizu, Y. Shirakami, H. Tsurumi, H. Moriwaki, Synergistic growth inhibition by 9-cis-retinoic acid plus trastuzumab in human hepatocellular carcinoma cells, Clin. Cancer Res. 14 (2008) 2806–2812.

[22] Y. Liu, Hepatoprotection by the farnesoid X receptor agonist GW4064 in rat models of intra- and extrahepatic cholestasis, J. Clin. Invest. 112 (2003) 1678–1687.

[23] I. Kim, S.H. Ahn, T. Inagaki, M. Choi, S. Ito, G.L. Guo, S.A. Kliewer, F.J. Gonzalez, Differential regulation of bile acid homeostasis by the farnesoid X receptor in liver and intestine, J. Lipid Res. 48 (2007) 2664–2672.

[24] C. Giordano, S. Catalano, S. Panza, D. Vizza, I. Barone, D. Bonofiglio, L. Gelsomino, P. Rizza, S.A. Fuqua, S. Ando, Farnesoid X receptor inhibits tamoxifen-resistant MCF-7 breast cancer cell growth through downregulation of HER2 expression, Oncogene (2011).

[25] K.E. Swales, M. Korbonits, R. Carpenter, D.T. Walsh, T.D. Warner, D. Bishop-Bailey, The farnesoid X receptor is expressed in breast cancer and regulates apoptosis and aromatase expression, Cancer Res. 66 (2006) 10120–10126.

[26] J. Kaeding, E. Bouchaert, J. Belanger, P. Caron, S. Chouinard, M. Verreault, O. Larouche, G. Pelletier, B. Staels, A. Belanger, O. Barbier, Activators of the farnesoid X receptor negatively regulate androgen glucuronidation in human prostate cancer LNCAP cells, Biochem. J. 410 (2008) 245–253.

[27] L. Zhao, M.G. Wientjes, J.L. Au, Evaluation of combination chemotherapy: integration of nonlinear regression, curve shift, isobologram, and combination index analyses, Clin. Cancer Res. 10 (2004) 7994–8004.

[28] M. Shimizu, Y. Yasuda, H. Sakai, M. Kubota, D. Terakura, A. Baba, T. Ohno, T. Kochi, H. Tsurumi, T. Tanaka, H. Moriwaki, Pitavastatin suppresses diethylnitrosamine-induced liver preneoplasms in male C57BL/KsJ-db/db obese mice, BMC Cancer 11 (2011) 281.

[29] M. Shimizu, M. Suzui, A. Deguchi, J.T. Lim, I.B. Weinstein, Effects of acyclic retinoid on growth, cell cycle control, epidermal growth factor receptor signaling, and gene expression in human squamous cell carcinoma cells, Clin. Cancer Res. 10 (2004) 1130–1140.

[30] Y. Zhang, P. Xu, K. Park, Y. Choi, D.D. Moore, L. Wang, Orphan receptor small heterodimer partner suppresses tumorigenesis by modulating cyclin D1 expression and cellular proliferation, Hepatology 48 (2008) 289–298.

[31] R.R. Maran, A. Thomas, M. Roth, Z. Sheng, N. Esterly, D. Pinson, X. Gao, Y. Zhang, V. Ganapathy, F.J. Gonzalez, G.L. Guo, Farnesoid X receptor deficiency in mice leads to increased intestinal epithelial cell proliferation and tumor development, J. Pharmacol. Exp. Ther. 328 (2009) 469–477.

[32] Y. Zhang, J. Soto, K. Park, G. Viswanath, S. Kuwada, E.D. Abel, L. Wang, Nuclear receptor SHP, a death receptor that targets mitochondria, induces apoptosis and inhibits tumor growth, Mol. Cell Biol. 30 (2010) 1341–1356.

[33] D.J. Mulholland, S. Dedhar, G.A. Coetzee, C.C. Nelson, Interaction of nuclear receptors with the Wnt/beta-catenin/Tcf signaling axis: Wnt you like to know?, Endocr Rev. 26 (2005) 898–915.

[34] Y. Yamada, Y. Shidoji, Y. Fukutomi, T. Ishikawa, T. Kaneko, H. Nakagama, M. Imawari, H. Moriwaki, Y. Muto, Positive and negative regulations of albumin gene expression by retinoids in human hepatoma cell lines, Mol. Carcinog. 10 (1994) 151–158.

[35] M. Suzui, M. Shimizu, M. Masuda, J.T. Lim, N. Yoshimi, I.B. Weinstein, Acyclic retinoid activates retinoic acid receptor beta and induces transcriptional activation of p21(CIP1) in HepG2 human hepatoma cells, Mol. Cancer Ther. 3 (2004) 309–316.

[36] M. Shimizu, H. Sakai, Y. Shirakami, J. Iwasa, Y. Yasuda, M. Kubota, K. Takai, H. Tsurumi, T. Tanaka, H. Moriwaki, Acyclic retinoid inhibits diethylnitrosamine-induced liver tumorigenesis in obese and diabetic C57BLKS/J- +(db)/+Lepr(db) mice, Cancer Prev. Res. 4 (2011) 128–136.

[37] H. Araki, Y. Shidoji, Y. Yamada, H. Moriwaki, Y. Muto, Retinoid agonist activities of synthetic geranyl geranoic acid derivatives, Biochem. Biophys. Res. Commun. 209 (1995) 66–72.

[38] T. Sano, M. Kagawa, M. Okuno, N. Ishibashi, M. Hashimoto, M. Yamamoto, R. Suzuki, H. Kohno, R. Matsushima-Nishiwaki, Y. Takano, H. Tsurumi, S. Kojima, S.L. Friedman, H. Moriwaki, T. Tanaka, Prevention of rat hepatocarcinogenesis by acyclic retinoid is accompanied by reduction in emergence of both TGF-alpha-expressing oval-like cells and activated hepatic stellate cells, Nutr. Cancer 51 (2005) 197–206.

[39] S. Fiorucci, S. Cipriani, A. Mencarelli, F. Baldelli, G. Bifulco, A. Zampella, Farnesoid X Receptor Agonist for the Treatment of Liver and Metabolic Disorders: Focus on 6-ethyl-CDCA, Mini Rev. Med. Chem. 11 (2011) 753–762.

Cancer Science
The official journal of the Japanese Cancer Association JCA

Suppression of azoxymethane-induced colonic preneoplastic lesions in rats by 1-methyltryptophan, an inhibitor of indoleamine 2,3-dioxygenase

Kengo Ogawa,[1] Takeshi Hara,[1] Masahito Shimizu,[1] Soranobu Ninomiya,[1] Junji Nagano,[1] Hiroyasu Sakai,[1] Masato Hoshi,[2] Hiroyasu Ito,[2] Hisashi Tsurumi,[1,5] Kuniaki Saito,[3] Mitsuru Seishima,[2] Takuji Tanaka[4] and Hisataka Moriwaki[1]

[1]First Department of Internal Medicine, Gifu University Graduate School of Medicine, Gifu; [2]Department of Informative Clinical Medicine, Gifu University Graduate School of Medicine, Gifu; [3]Human Health Sciences, Graduate School of Medicine and Faculty of Medicine, Kyoto University, Kyoto; [4]The Tohkai Cytopathology Institute, Cancer Research and Prevention (TCI-CaRP), Gifu, Japan

(Received November 29, 2011/Revised February 3, 2012/Accepted February 4, 2012/Accepted manuscript online February 9, 2012/Article first published online March 6, 2012)

The escape of preneoplastic cells from the immune system, which is caused by immune tolerance, occurs during the development of several types of tumors. Indoleamine 2,3-dioxygenase (IDO) plays a critical role in the induction of immune tolerance. In the present study we investigated the effects of 1-methyltryptophan (1-MT), an IDO inhibitor, and (–)-epigallocatechin gallate (EGCG), the major catechin in green tea, on the development of azoxymethane (AOM)-induced colonic preneoplastic lesions by focusing on the inhibition of IDO. To induce colonic premalignant lesions, male F344 rats were injected with AOM (20 mg/kg body weight, s.c.) once a week for 2 weeks. They also received 0.2% 1-MT or 0.1% EGCG in their drinking water for 4 weeks, starting 1 week before the first dose of AOM. Both 1-MT and EGCG significantly decreased the total number of aberrant crypt foci and β-catenin-accumulated crypts, which overexpressed IDO protein. Treatment with EGCG decreased IDO mRNA expression in both the colonic epithelium and stroma of rats induced by AOM. The AOM-induced increase in *cyclooxygenase-2* mRNA expression in the colonic stroma was significantly decreased by EGCG. Furthermore, AOM-induced increases in IDO activity in the serum and stroma were significantly inhibited by 1-MT and EGCG. Inhibition of IDO activity by 1-MT and EGCG was also observed in cell-free assays. These findings suggest that upregulation of IDO activity is observed in the early stages of colon carcinogenesis and that the use of IDO inhibitors, such as 1-MT and EGCG, which suppress the occurrence of colonic preneoplastic lesions, could be a novel strategy for the chemoprevention of colon cancer. (*Cancer Sci* 2012; 103: 951–958)

The immune system recognizes preneoplastic cells and, in most cases, eliminates these cells before they expand into clinically detectable tumors. Therefore, the escape of precancerous cells from the immune system, which is closely associated with immune tolerance, is involved in the development of several types of tumors.[1] Recent studies have suggested that indoleamine 2,3-dioxygenase (IDO) plays a crucial role in the induction of immune tolerance.[2] Indoleamine 2,3-dioxygenase is an intracellular enzyme that catalyses the first and rate-limiting steps in the catabolism of the essential amino acid tryptophan along the kynurenine pathway.[3] In the tumor microenvironment, increased IDO activity inhibits the proliferation of T and natural killer cells and induces apoptosis through tryptophan depletion and the production of toxic tryptophan catabolites.[4] Overexpression of IDO has been shown to be correlated with poor clinical outcome in patients with ovarian carcinoma, endometrial carcinoma, and colorectal carcinoma.[5–7] We have recently reported that, in diffuse large B-cell lymphoma, IDO expression in tumor cells and serum concentrations of L-kynurenine, which reflect IDO activity, are useful indicators of a poor prognosis.[8,9] Several preclinical studies using rodent cancer models have demonstrated that IDO inhibitors, such as 1-methyltryptophan (1-MT), are therapeutically beneficial, especially when combined with different types of cytotoxic chemotherapeutic agents.[10,11] These reports suggest that targeting IDO, and therefore regulating tryptophan catabolism, may be an effective strategy for the treatment of certain types of human malignancies.[12] However, the possibility of cancer chemoprevention by inhibiting IDO expression and/or activity has not been considered.

(−)-Epigallocatechin gallate (EGCG), one of the major catechins in green tea, is the most biologically active component of green tea. It has been shown to exert its cancer chemopreventive and anti-carcinogenic effects in various organs, including the colon.[13,14] Previously, we demonstrated that EGCG can inhibit the growth of and induce apoptosis in human colorectal cancer cells.[15–17] The inhibitory effects of EGCG on both inflammation- and obesity-related colon carcinogenesis have also been demonstrated.[18,19] In addition, green tea polyphenols in the drinking water have been shown to inhibit the development of putative preneoplastic lesions called aberrant crypt foci (ACF) in rats treated with azoxymethane (AOM), which induces ACF.[20–22]

Recently, it was been reported that EGCG administration suppresses the expression of IDO in interferon (IFN)-γ-stimulated murine dendritic cells[23] and human oral cancer cell lines.[24] Although the mechanisms underlying the role of IDO in carcinogenesis have not yet been clarified, we hypothesized that the inhibitory effect of EGCG on IDO expression may contribute to the anti-carcinogenic properties of EGCG. To confirm our hypothesis, we examined the effects of 1-MT and EGCG on the development in the colon of AOM-induced preneoplastic lesions, namely ACF[21] and β-catenin-accumulated crypts (BCAC),[25] in male F344 rats by focusing on the inhibition of IDO expression and activity.

Materials and Methods

Animals, chemicals, and diets. Male F344 rats, aged 4 weeks (Charles River Japan, Tokyo, Japan), were maintained at the Gifu University Animal Facility according to Institutional Animal Care Guidelines. All rats were housed in plastic cages with free access to drinking water and a pelleted basal diet

[5]To whom correspondence should be addressed.
E-mail: htsuru@gifu-u.ac.jp

doi: 10.1111/j.1349-7006.2012.02237.x
© 2012 Japanese Cancer Association

(CRF-1; Oriental Yeast, Tokyo, Japan). Both 1-MT and AOM were purchased from Sigma (St Louis, MO, USA), whereas EGCG was obtained from Mitsui Norin (Tokyo, Japan). For 1-MT and EGCG treatment of rats, 1-MT (0.2%) and EGCG (0.1%) solutions were prepared in tap water and administered to the rats in their drinking water *ad libitum*. Fresh test solutions were prepared three times a week. The concentration of EGCG (0.1%) used in the present study was chosen on the basis of the results of previous chemopreventive studies[19,26] and was within the physiologic range of the daily intake of green tea catechins in humans on a per unit body weight basis.[27]

Experimental procedure

As shown in Figure 1, 60 male F344 rats were quarantined for the first 7 days and then randomized into one of three groups to receive either 0.2% 1-MT, 0.1% EGCG, or no test compounds. One week later, the rats in each group were further grouped to receive subcutaneous injections of AOM (20 mg/kg body weight) or saline (200 μL) once a week for 2 weeks. Rats were given control and test drinking water for 4 weeks, starting 1 week before the first AOM injection. All measurements, including the large bowel excision and the collection of blood samples from the inferior vena cava, were performed from rats that had been killed by CO_2 asphyxiation at Week 4 (9 weeks of age). One-quarter of the excised colons (cecum side) was used for crypt isolation, whereas the remainder was used to determine the number of colonic ACF and BCAC (see below). After the number of ACF had been counted, the colon was rolled like a "Swiss roll"[28] and paraffin-embedded sections were prepared using routine procedures for subsequent histopathologic and immunohistochemical examinations.

Counting colonic ACF and BCAC. The number of ACF and BCAC was determined as described previously.[25,29,30] Briefly, buffered formalin-fixed colons were stained with 0.5% methylene blue solution for 20 s and then placed on microscope slides to count the number of ACF and to determine their size. The number of ACF in the colon was recorded along with the number of crypts in each focus and the data are expressed as the total number of ACF per colon, total number of aberrant crypts (ACs) per colon, number of ACs per focus, and total number of large ACF (i.e. ACF with four or more aberrant crypts) per colon.[29] After the number of ACF had been counted, the rectal mucosa (2.0 cm from the anus) was cut and embedded in paraffin to identify BCAC intramucosal lesions, with 4-μm sections obtained from an *en face* preparation. The number of BCAC on histological sections stained with β-catenin was counted and is expressed as the number of BCAC per cm^2 mucosa.

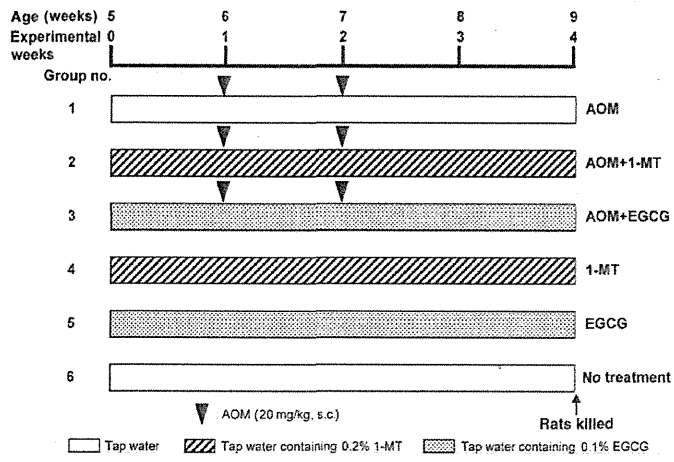

Fig. 1. Experimental protocol. Rats (5 weeks old) were allocated to one of six groups and treated over a period of 4 weeks, as indicated. AOM, azoxymethane; 1-MT, 1-methyltryptophan; EGCG, (−)-epigallocatechin gallate.

Immunohistochemical analysis. After endogenous peroxidase activity had been blocked with H_2O_2, sections were incubated overnight at 4°C with primary antibodies: anti-β-catenin (1:1000; BD Biosciences PharMingen, San Diego, CA, USA), anti-IDO (1:1000; LYFESPAN, Seattle, WA, USA), and anti-L-kynurenine (1:1000; Abnova, Taipei City, Taiwan). Subsequently, sections for the immunohistochemistry of β-catenin and IDO were incubated with biotinylated secondary antibodies against the primary antibodies (DAKO, Carpinteria, CA, USA), followed by incubation with avidin-coupled peroxidase. The sections for L-kynurenine immunohistochemistry were incubated with peroxidase-labeled polymer-conjugated secondary antibodies against the primary antibodies. They were then developed with 3,3′-diaminobenzidine using DAKO Liquid DAB Substrate-Chromogen System (DAKO) and counterstained with hematoxylin.

Crypt isolation. Colonic tissue was washed twice with 1 × Hank's balanced salt solution (HBSS; Sigma) and then incubated with 1 × HBSS containing 30 mM EDTA at 37°C for 15 min. The tissue was dispersed in 1 × HBSS solution by vortexing and separated into epithelial crypts and stromal tissues as described previously.[31]

Quantitative real-time RT-PCR. Total RNA was extracted from isolated epithelial crypts and stromal tissues using the RNeasy Mini Kit (Qiagen, Hilden, Germany). Total RNA (1 μg) was used for the synthesis of first-strand cDNA. Quantitative real-time RT-PCR was performed using specific primer/probe sets that amplified the *IDO*, *tryptophan 2,3-dioxygenase* (*TDO*), *cyclooxygenase* (*COX*)-2, *IFN-γ*, and *GAPDH* genes (TaqMan Gene Expression Assays; Applied Biosystems, Foster City, CA, USA) and TOYOBO Real-time PCR Master Mix (TOYOBO, Osaka, Japan). Each sample was analyzed on a LightCycler 1.0 (Roche Diagnostics, Mannheim, Germany), as described previously.[32] The expression of each gene was normalized against that of *GAPDH* using the standard curve method.

Determination of IDO activity. Indoleamine 2,3-dioxygenase activity was determined by calculating the ratio of L-kynurenine/L-tryptophan in serum and colonic tissues.[33] Serum samples were deproteinized with 3% perchloric acid. Isolated epithelial crypt and stromal samples were homogenized in 2 μL of 3% perchloric acid per mg tissue. After centrifugation at 4°C and 20 000 *g* for 10 min, aliquots of the supernatant were collected for HPLC determination of L-tryptophan and L-kynurenine concentrations, as described previously.[34]

The enzymatic activity of IDO was also measured using cell-free assays. An aliquot of recombinant human IDO (R&D Systems, Minneapolis, MN, USA) was diluted in 50 mM 2-(*N*-morpholino)ethanesulfonic buffer (pH 6.5). The reaction mixture contained 50 μL enzyme preparation and 50 μL substrate solution, which consisted of 100 mM potassium phosphate buffer (pH 6.5), 50 μM methylene blue, 20 μg catalase, 50 mM ascorbate, 0.4 mM L-tryptophan, and 2000 μM 1-MT or 200 μM EGCG. After incubation of the reaction mixture at 37°C for 1 h, the concentrations of the enzymatic products were measured by HPLC.[35] Enzymatic activity is expressed as the product content per hour.

Statistical analysis. All data are expressed as the mean ± SD. Differences between groups were analyzed by two-way ANOVA and, when statistical significance was found, individual

doi: 10.1111/j.1349-7006.2012.02237.x
© 2012 Japanese Cancer Association

differences were evaluated using the Tukey–Kramer multiple comparison test. $P < 0.05$ was considered significant.

Results

General observations. All rats remained healthy and none died during the experimental period. There were no significant differences in the consumption of food (data not shown) and drinking water (Table 1) between the different groups. Body, liver, and relative liver weights, as well as the length of the large bowel, at the end of the study are given in Table 1. The mean body weight of the AOM + 1-MT group was only significantly less than that of the 1-MT group ($P < 0.05$). This decrease may have been due to AOM toxicity, as observed in previous studies,[19,36,37] because 1-MT alone did not reduce body weight in the absence of AOM. Other measurements did not differ significantly among the groups. Histopathologically, there were no findings suggesting toxicity of 1-MT or EGCG in the liver, kidney, or spleen of rats (data not shown).

Effects of 1-MT and EGCG on AOM-induced ACF and BCAC in F344 rats. All rats in the AOM, AOM + 1-MT, and AOM + EGCG groups (i.e. all those treated with AOM) developed ACF and BCAC. In the 1-MT, EGCG, and untreated groups, there were no microscopically observable changes, including ACF or BCAC, in the colon. Compared with the group treated with AOM alone, daily oral administration of 1-MT and EGCG in the drinking water significantly reduced the frequency of ACF ($P < 0.001$ for each comparison). The reduction in the frequency of ACF was significantly greater following EGCG administration than after 1-MT administration ($P < 0.05$). We also noticed a significant reduction in the percentage of large ACF, consisting of four or more aberrant crypts, in the AOM + 1-MT and AOM + EGCG groups compared with the AOM group ($P < 0.001$ for each comparison; Fig. 2a). In addition, the number of BCAC per cm^2 in the AOM + 1-MT and AOM + EGCG groups was significantly less than that in the AOM group ($P < 0.001$ for each comparison; Fig. 2b).

Immunohistochemical analysis of IDO and L-kynurenine in the colonic mucosa. The expression of IDO and L-kynurenine was determined in colonic crypts and preneoplastic lesions (i.e. ACF and BCAC) using immunohistochemical analysis. Compared with colonic crypt cells in untreated control rats, which exhibited only weak positive cytoplasmic staining to IDO, there was a significant increase in IDO staining in the atypical cell cytoplasm of the ACF and BCAC that had developed in AOM-treated rats. Furthermore, L-kynurenine expression, which was very weak in normal crypts of untreated control rats, was slightly increased in the ACF and BCAC of AOM-treated rats (Fig. 3a). Neither EGCG nor 1-MT treatment significantly altered the AOM-induced increases in IDO and L-kynurenine staining (Fig. 3b,c).

Effects of 1-MT and EGCG on IDO and TDO expression in isolated epithelial crypts and stromal cells. In cancer tissues, IDO is overexpressed in both tumor epithelial cells and antigen-presenting cells in the stroma.[38] Tryptophan 2,3-dioxygenase, a hepatic enzyme that catalyses the first step of tryptophan degradation, is also expressed in many tumors.[39] Therefore, after crypt isolation, we determined whether there was increased expression of IDO and TDO in both epithelial crypts and stromal tissues in the colon of AOM-treated rats. As indicated in Figure 4(a,b), quantitative RT-PCR analysis revealed a significant increase in IDO expression in both the crypts and stromal cells of the AOM-treated group compared with the untreated control group ($P < 0.05$ for each comparison). Furthermore, these increases were significantly inhibited by EGCG treatment ($P < 0.05$ for each comparison). Although 1-MT treatment tended to decrease IDO expression in crypts and stromal tissues, the difference failed to reach statistical significance. In the absence of AOM treatment, *IDO* mRNA expression was not affected by the administration of either 1-MT or EGCG. In contrast with IDO, AOM did not induce an increase in *TDO* mRNA expression and neither EGCG nor 1-MT had any effect on TDO expression in crypts and stromal tissues (Fig. 4c,d).

Effects of 1-MT and EGCG on IDO activity. We next examined the enzymatic activity of IDO in serum and colon tissues of AOM-treated rats by measuring the concentrations of L-kynurenine and L-tryptophan. The L-kynurenine/L-tryptophan ratios in the serum (Fig. 5a) and stromal cells (Fig. 5c) of the AOM-treated group were significantly higher than in the untreated control group ($P < 0.05$ for each comparison). Treatment of rats with 1-MT and EGCG resulted in a significant decrease in these ratios in AOM-treated rats ($P < 0.05$ for each comparison), suggesting that 1-MT and EGCG significantly inhibit both the systemic (serum) and focal (colonic stromal) AOM-induced increases in IDO activity. In epithelial cells, there were no significant differences in the L-kynurenine/L-tryptophan ratios between the different groups (Fig. 5b). In the absence of AOM treatment, neither 1-MT nor EGCG alone had any effect on the L-kynurenine/L-tryptophan ratios (Fig. 5a–c).

To further investigate whether 1-MT and EGCG directly influence IDO activity, we measured IDO enzyme kinetics (kynurenine production) using recombinant human IDO in a cell-free system. As shown in Figure 6, levels of L-kynurenine produced by IDO were significantly inhibited by 1-MT and EGCG treatment ($P < 0.001$ for each comparison). These findings suggest that both 1-MT and EGCG act directly to inhibit IDO activity.

Effects of 1-MT and EGCG on COX-2 and IFN-γ expression in stromal cells. We next assessed the inhibitory effects of 1-MT and EGCG on COX-2 and IFN-γ expression, because both are regulated by inflammatory cells in the stroma and are implicated in the induction of IDO.[40–43] Using quantitative RT-PCR, we found that the expression of *COX-2* mRNA in stromal tissues was markedly upregulated in the AOM-treated group, but this upregulation was significantly inhibited by

Table 1. General parameters

Treatment	No. rats examined	Drinking water intake (g/day)	Body weight (g)	Liver weight (g)	Relative liver weight (g/100 g body weight)	Length of the large bowel (cm)
AOM alone	14	27.3 ± 1.3	203 ± 11	10.2 ± 1.0	5.0 ± 0.5	19.0 ± 1.8
AOM + 0.2% 1-MT	14	25.2 ± 2.3	198 ± 13*	10.1 ± 0.7	5.1 ± 0.4	19.6 ± 1.1
AOM + 0.1% EGCG	14	26.1 ± 2.9	202 ± 8	9.8 ± 0.8	4.9 ± 0.5	19.0 ± 0.9
0.2% 1-MT	6	25.3 ± 4.3	217 ± 12	10.6 ± 0.8	4.9 ± 0.2	20.3 ± 1.6
0.1% EGCG	6	26.5 ± 1.4	212 ± 16	10.2 ± 0.9	4.8 ± 0.6	19.5 ± 1.1
No treatment	6	26.8 ± 0.8	208 ± 9	9.6 ± 0.8	4.6 ± 0.4	19.0 ± 2.1

Data are given as the mean ± SD. *P < 0.05 compared with 0.2% 1-methyltryptophan (1-MT) alone. AOM, azoxymethane; EGCG, (–)-epigallocatechin gallate.

© 2012 Japanese Cancer Association

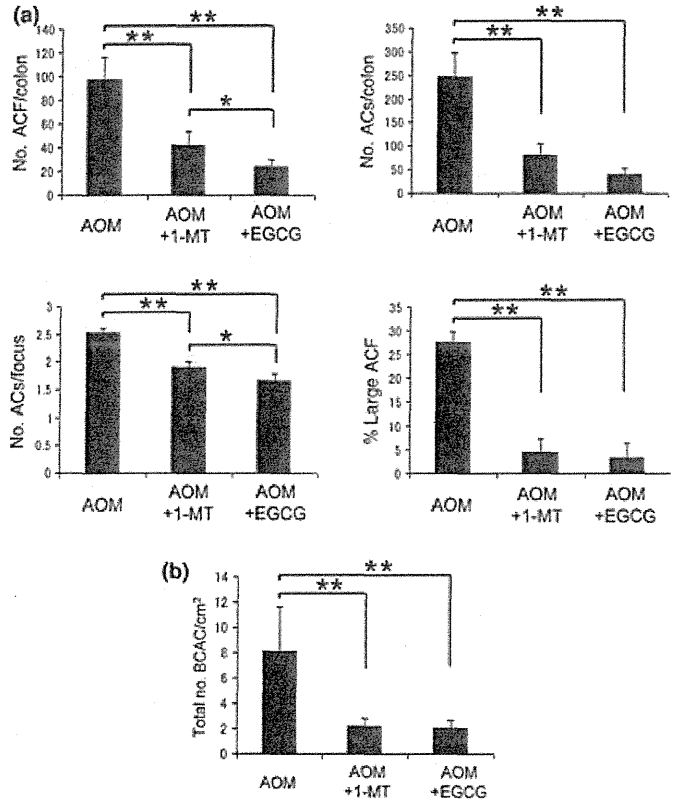

Fig. 2. Effects of 1-methyltryptophan (1-MT) and (−)-epigallocatechin gallate (EGCG) on azoxymethane (AOM)-induced formation of aberrant crypt foci (ACF) and β-catenin-accumulated crypts (BCAC). (a) Number of ACF per colon, total number of aberrant crypts (ACs) per colon, the number of ACs in each focus, and the percentage of large ACF (i.e. those with four or more ACs). (b) Number of BCAC per cm^2. Data are the mean ± SD (n = 6). *P < 0.05, **P < 0.001.

EGCG treatment (Fig. 7a). In addition, although AOM increased *IFN-γ* mRNA expression in stromal cells, this increase was not inhibited by EGCG (Fig. 7b). Treatment of rats with 1-MT did not have any significant effect on AOM-induced increases in the expression of *COX-2* or *IFN-γ* mRNA. In the absence of AOM treatment, neither 1-MT nor EGCG alone had any effect on *COX-2* or *IFN-γ* mRNA levels (Fig. 7a,b).

Discussion

The results of the present study suggest that upregulation of IDO is possibly involved in colon carcinogenesis, as evidenced by higher IDO expression (Figs 3a,4a,b) and activity (Fig. 5c) in the colonic mucosa of AOM-treated rats compared with the untreated controls, which did not receive any carcinogen. The results of the present study also provide the first evidence that treatment with the IDO inhibitor 1-MT effectively suppresses the development of colonic preneoplastic lesions (ACF and BCAC) induced by AOM (Fig. 2). This inhibition is considered to be associated with the inhibition of IDO activity, which is increased in AOM-treated rats (Fig. 5a,c), because IDO-mediated immune tolerance plays a critical role in tumor development and progression.[2,3] Therefore, 1-MT may correct IDO-mediated immune escape and thus suppress AOM-induced colorectal carcinogenesis. These results suggest that upregulation of IDO, and most likely subsequent immune tolerance caused by this enzyme, is involved in the early phase of colon carcinogenesis and that targeting IDO may, therefore, be an effective strategy to prevent colorectal carcinogenesis.

The chemopreventive and anti-cancer effects of green tea and EGCG are partially attributed to their anti-oxidative properties, their anti-angiogenic and anti-mutagenic effects, and their anti-inflammatory activities, all of which act in combination to suppress carcinogenesis. Thus, these activities are considered to be the main mechanisms underlying the anti-cancer effects of EGCG.[13,14] Furthermore, earlier studies showed

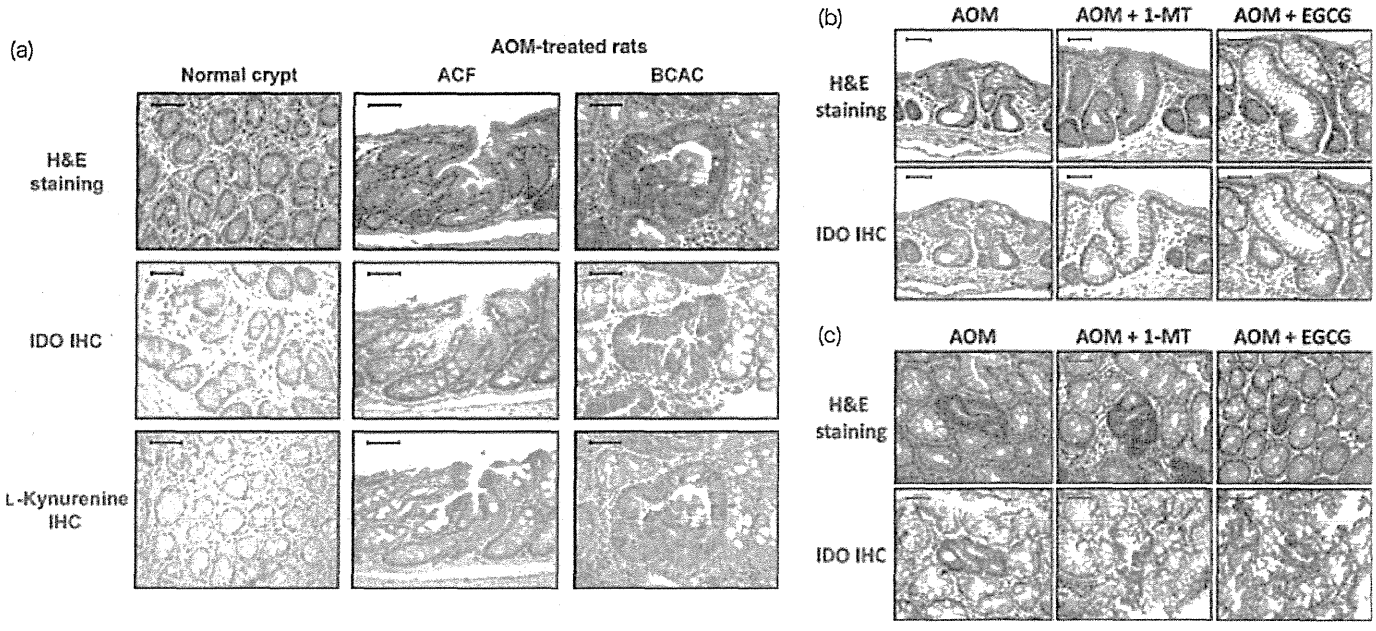

Fig. 3. Immunohistochemical evaluation of the expression of indoleamine 2,3-dioxygenase (IDO) and L-kynurenine in normal crypts from untreated rats and aberrant crypt foci (ACF), and β-catenin-accumulated crypts (BCAC) in the colonic mucosa of rats treated with azoxymethane (AOM). (a) Expression of IDO and L-kynurenine in representative samples of colonic mucosa, as evidenced by H&E staining and immunohistochemistry (IHC). (b,c) Effects of 1-methyltryptophan (1-MT) and (−)-epigallocatechin gallate (EGCG) on the expression of IDO in ACF (b) and BCAC (c), as determined by IHC. Scale lines, 50 μm.

doi: 10.1111/j.1349-7006.2012.02237.x
© 2012 Japanese Cancer Association

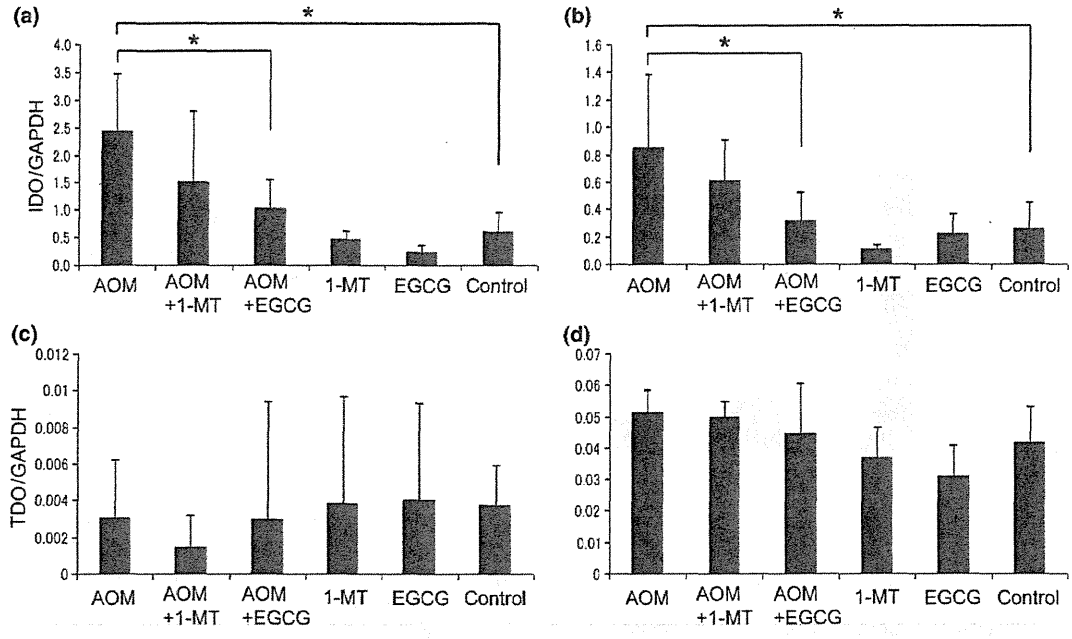

Fig. 4. Effects of 1-methyltryptophan (1-MT) and (−)-epigallocatechin gallate (EGCG) on the expression of (a,b) indoleamine 2,3-dioxygenase (IDO) and (c,d) tryptophan 2,3-dioxygenase (TDO) in the epithelium (a,c) and stroma (b,d). Total RNA was extracted from epithelial crypts and stromal tissues and IDO and TDO mRNA expression evaluated by quantitative RT-PCR. Expression is normalized against that of GAPDH. AOM, azoxymethane. Data are the mean ± SD (n = 6). *P < 0.05.

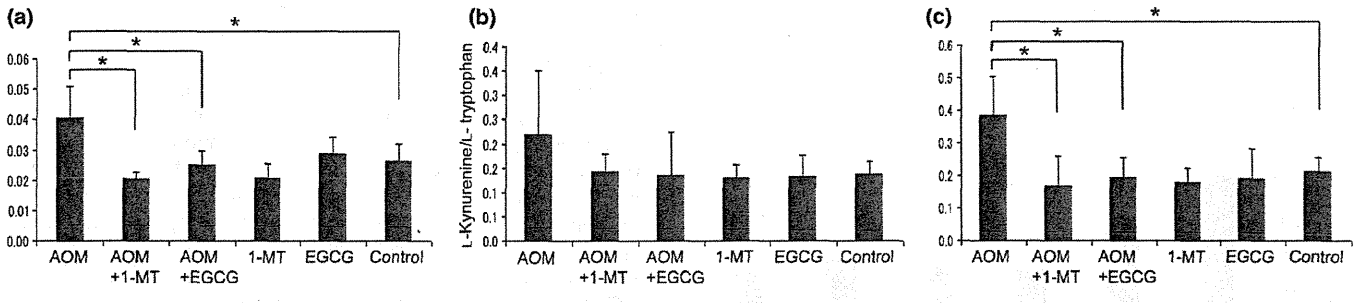

Fig. 5. Effects of 1-methyltryptophan (1-MT) and (−)-epigallocatechin gallate (EGCG) on indoleamine 2,3-dioxygenase (IDO) activity in the (a) serum and colonic (b) epithelium and (c) stroma. Functional IDO activity was determined by measuring the concentrations of L-kynurenine and tryptophan using HPLC. The L-kynurenine/L-tryptophan ratio indicates IDO activity. AOM, azoxymethane. Data are the mean ± SD (n = 6). *P < 0.05.

that EGCG suppresses the induction of IDO *in vitro*.[23,24] In the present study, EGCG inhibited the functional enzyme activity of IDO in AOM-treated rats (Fig. 5a,c). In addition, the inhibitory effects of EGCG against AOM-induced increases in *IDO* mRNA expression in the colonic mucosa were greater than those of 1-MT (Fig. 4a,b). This may be associated with the observation that EGCG caused a greater inhibition of the total number of ACF that did 1-MT (Fig. 2a). Therefore, these results suggest that, in addition to the previously reported multiple critical mechanisms of action underlying tumor suppression,[13,14] EGCG may prevent the early phase of colon carcinogenesis, at least in part, by inhibiting the expression and activity of IDO and thus mediating an immune response. The results of a recent study indicating that green tea catechins exert anti-cancer effects by regulating the expression and function of both T and natural killer cells[44] may also strengthen the case for EGCG modulating immune tolerance.

A recent study has revealed the possible roles of toxic tryptophan catabolites produced by IDO in cancer.[45] Of these metabolites, L-kynurenine is considered to play a critical role in the immune escape of malignant cells that occurs within the tumor and its surrounding microenvironment.[4] Conversely, IDO inhibitors can impede the growth of IDO-expressing tumors by reducing the amount of kynurenine present in the microenvironment.[46] Therefore, in addition to inhibiting IDO expression, EGCG has a direct effect in inhibiting IDO enzyme activity (Fig. 6), which may have contributed to its prevention of the development of colonic preneoplastic lesions in the present study.

In the present study, *IDO* mRNA levels in both the epithelium and stroma decreased in rats treated with 1-MT or EGCG; however, the ratio of L-kynurenine/L-tryptophan decreased only in the stroma (Fig. 4a,b,5c). These findings suggest that IDO-induced metabolic conversion of tryptophan to kynurenine occurs mainly in the stroma. For example, in human dendritic cells constitutively expressing IDO protein, the functional activity of this enzyme is tightly regulated and requires additional triggering signals supplied during antigen presentation by $CD4^+$ T cells.[47] Many important immunoregulatory pathways, such as the IFN/JAK/signal transducer and activator of transcription (STAT) pathway and the non-canonical nuclear factor-κB pathway, which are controlled by

© 2012 Japanese Cancer Association

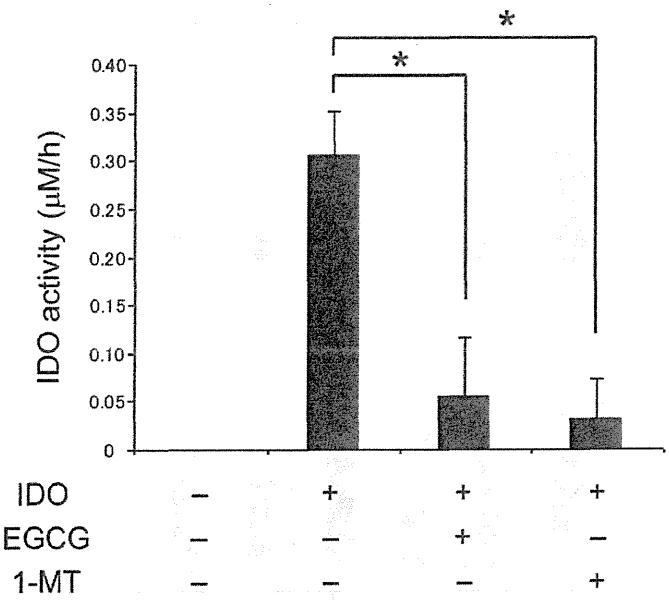

Fig. 6. Effects of 1-methyltryptophan (1-MT) and (−)-epigallocatechin gallate (EGCG) on indoleamine 2,3-dioxygenase (IDO) activity in cell-free assays. Functional activity of recombinant human IDO enzyme in response to 1-MT and EGCG was determined by measuring the concentrations of enzymatic products (L-kynurenine) using HPLC. Enzymatic activity is expressed as the product content per hour (μM/h). Data are the mean ± SD. *P < 0.001.

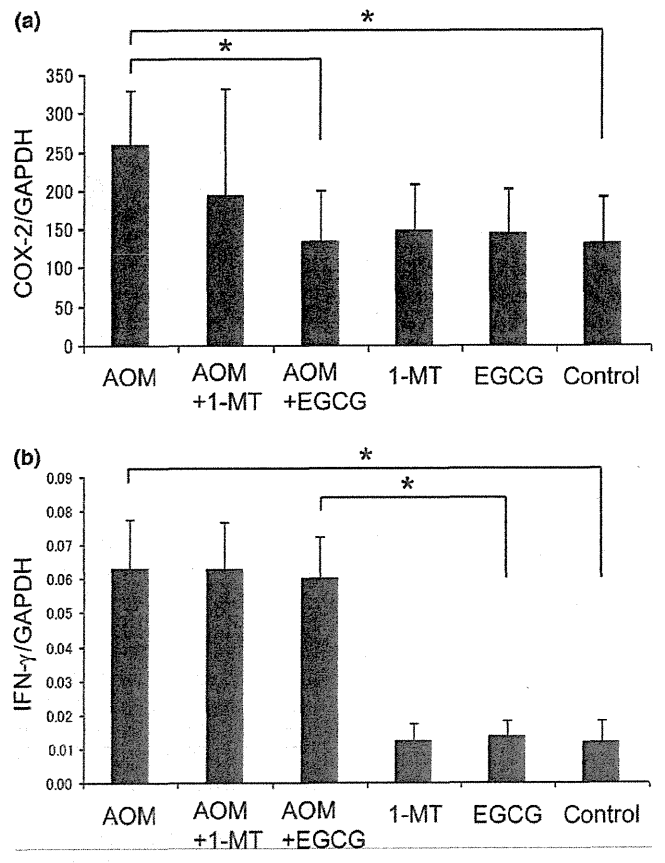

Fig. 7. Effects of 1-methyltryptophan (1-MT) and (−)-epigallocatechin gallate (EGCG) on the expression of (a) cyclooxygenase (COX)-2 and (b) interferon (IFN)-γ in stromal cells, as determined by quantitative RT-PCR. Expression is normalized against that of GAPDH. AOM, azoxymethane. Data are the mean ± SD (n = 6). *P < 0.05.

immune cells in the stroma, are related to IDO expression.[38] In addition, several other immune regulatory factors have been implicated as inducers of IDO, including COX-2, which is regarded as one of the most critical inflammatory mediators in the regulation of IDO expression.[42] In the present study, the AOM-induced upregulation of COX-2 in the colonic stroma of rats was significantly inhibited by the administration of EGCG (Fig. 7a). These findings, together with those of Basu *et al.*,[43] who reported a suppressive role of a COX-2 inhibitor against IDO expression in the tumor microenvironment, suggest that EGCG inhibits the expression of IDO, possibly by preventing the induction of COX-2, although further investigations are required to clarify the effects of EGCG. Thus, combination treatment using an IDO inhibitor plus a COX-2 inhibitor may be an effective regimen for the chemoprevention of colorectal cancer because this combination will synergistically inhibit the expression and activity of IDO.

Interferon-γ is also thought to be a major stimulator of IDO,[40,41] and EGCG has been reported to suppress IDO expression by inhibiting STAT-1 activation in response to IFN-γ *in vitro*.[23,24] However, in the present study the expression of IFN-γ in the colonic stroma was not affected by EGCG in the drinking water (Fig. 7b). Other novel mechanisms by which EGCG modulates the expression of IDO may exist; therefore, further studies are needed to clarify the effects of EGCG on the immunoregulatory pathways related to IDO expression.

Aberrant crypt foci have attracted attention as putative precancerous lesions of the colon in experimental models.[48] Numerous molecular abnormalities, including increased expression of K-*ras* and *APC* gene mutations, have been demonstrated in human ACF.[49] In addition, BCAC, which accumulate β-catenin protein in the nucleus and cytoplasm, are regarded as putative precursors to colorectal adenomas.[50] Several rodent studies have shown that both these lesions are useful as biomarkers to evaluate the chemopreventive properties of specific agents.[19,36,37,51] Therefore, our findings, namely that both 1-MT and EGCG markedly inhibit the development of ACF and BCAC, appear to be significant when considering the chemoprevention of colorectal cancer. In particular, a significant reduction of large ACF by 1-MT and EGCG should be emphasized, because large ACF are known to have a strong correlation with the incidence of colonic adenocarcinoma.[20,21]

Finally, it should be mentioned that one limitation of the present study was that the L-kynurenine/L-tryptophan ratio may not directly reflect IDO activity because kynurenine can be metabolized further and TDO can also produce kynurenine from tryptophan.[12] However, in the present study we presumed that TDO exerted little effect on L-kynurenine levels because the expression of TDO was not affected by AOM treatment (Fig. 4c,d). Systemic IDO activity is currently estimated by the serum L-kynurenine/L-tryptophan ratio,[33] as in the present study, because IDO is an intracellular enzyme and circulating IDO concentrations are barely detectable.[3] In fact, a method for analyzing serum IDO protein itself has not been established in experimental animals and there is only one report, published in 2012, of its detection in humans.[52] This limitation needs to be addressed in future studies.

In conclusion, the escape of precancerous cells from the immune system caused by immune tolerance is involved in certain types of carcinogenesis and, therefore, may be an effective target for the implementation of chemoprevention. The results of the present study support the notion that IDO upregulation, which induces immune tolerance, contributes to the early phase of colon carcinogenesis. Furthermore, the present study is the first to provide evidence that the anti-carcinogenic properties of 1-MT and EGCG may be related to inhibition of

doi: 10.1111/j.1349-7006.2012.02237.x
© 2012 Japanese Cancer Association

IDO activity, suggesting that targeting IDO and correcting IDO-mediated immune tolerance with EGCG or an IDO inhibitor could be a promising strategy for the prevention of colorectal cancer development in the future. Further experiments using IDO-knockout mice would strengthen the connection between IDO activity and the development of colorectal cancer, and may prove useful in the exploration of IDO inhibitors as chemopreventive agents for colorectal cancer.

Acknowledgment

The authors thank Mitsui Norin (Tokyo, Japan) for providing the EGCG.

Disclosure Statement

The authors have no conflicts of interest to declare.

References

1 Zitvogel L, Tesniere A, Kroemer G. Cancer despite immunosurveillance: immunoselection and immunosubversion. *Nat Rev Immunol* 2006; 6: 715–27.
2 Uyttenhove C, Pilotte L, Theate I *et al.* Evidence for a tumoral immune resistance mechanism based on tryptophan degradation by indoleamine 2,3-dioxygenase. *Nat Med* 2003; 9: 1269–74.
3 Mellor AL, Munn DH. IDO expression by dendritic cells: tolerance and tryptophan catabolism. *Nat Rev Immunol* 2004; 4: 762–74.
4 Frumento G, Rotondo R, Tonetti M, Damonte G, Benatti U, Ferrara GB. Tryptophan-derived catabolites are responsible for inhibition of T and natural killer cell proliferation induced by indoleamine 2,3-dioxygenase. *J Exp Med* 2002; 196: 459–68.
5 Okamoto A, Nikaido T, Ochiai K *et al.* Indoleamine 2,3-dioxygenase serves as a marker of poor prognosis in gene expression profiles of serous ovarian cancer cells. *Clin Cancer Res* 2005; 11: 6030–9.
6 Ino K, Yoshida N, Kajiyama H *et al.* Indoleamine 2,3-dioxygenase is a novel prognostic indicator for endometrial cancer. *Br J Cancer* 2006; 95: 1555–61.
7 Brandacher G, Perathoner A, Ladurner R *et al.* Prognostic value of indoleamine 2,3-dioxygenase expression in colorectal cancer: effect on tumor-infiltrating T cells. *Clin Cancer Res* 2006; 12: 1144–51.
8 Ninomiya S, Hara T, Tsurumi H *et al.* Indoleamine 2,3-dioxygenase in tumor tissue indicates prognosis in patients with diffuse large B-cell lymphoma treated with R-CHOP. *Ann Hematol* 2010; 90: 409–16.
9 Yoshikawa T, Hara T, Tsurumi H *et al.* Serum concentration of L-kynurenine predicts the clinical outcome of patients with diffuse large B-cell lymphoma treated with R-CHOP. *Eur J Haematol* 2010; 84: 304–9.
10 Muller AJ, DuHadaway JB, Donover PS, Sutanto-Ward E, Prendergast GC. Inhibition of indoleamine 2,3-dioxygenase, an immunoregulatory target of the cancer suppression gene *Bin1*, potentiates cancer chemotherapy. *Nat Med* 2005; 11: 312–9.
11 Hou DY, Muller AJ, Sharma MD *et al.* Inhibition of indoleamine 2,3-dioxygenase in dendritic cells by stereoisomers of 1-methyl-tryptophan correlates with antitumor responses. *Cancer Res* 2007; 67: 792–801.
12 Lob S, Konigsrainer A, Rammensee HG, Opelz G, Terness P. Inhibitors of indoleamine-2,3-dioxygenase for cancer therapy: can we see the wood for the trees? *Nat Rev Cancer* 2009; 9: 445–52.
13 Yang CS, Maliakal P, Meng X. Inhibition of carcinogenesis by tea. *Annu Rev Pharmacol Toxicol* 2002; 42: 25–54.
14 Yang CS, Wang X, Lu G, Picinich SC. Cancer prevention by tea: animal studies, molecular mechanisms and human relevance. *Nat Rev Cancer* 2009; 9: 429–39.
15 Shimizu M, Deguchi A, Lim JT, Moriwaki H, Kopelovich L, Weinstein IB. (−)-Epigallocatechin gallate and polyphenon E inhibit growth and activation of the epidermal growth factor receptor and human epidermal growth factor receptor-2 signaling pathways in human colon cancer cells. *Clin Cancer Res* 2005; 11: 2735–46.
16 Shimizu M, Deguchi A, Joe AK, McKoy JF, Moriwaki H, Weinstein IB. EGCG inhibits activation of HER3 and expression of cyclooxygenase-2 in human colon cancer cells. *J Exp Ther Oncol* 2005; 5: 69–78.
17 Shimizu M, Deguchi A, Hara Y, Moriwaki H, Weinstein IB. EGCG inhibits activation of the insulin-like growth factor-1 receptor in human colon cancer cells. *Biochem Biophys Res Commun* 2005; 334: 947–53.
18 Shirakami Y, Shimizu M, Tsurumi H, Hara Y, Tanaka T, Moriwaki H. EGCG and polyphenon E attenuate inflammation-related mouse colon carcinogenesis induced by AOM and DSS. *Mol Med Report* 2008; 1: 355–61.
19 Shimizu M, Shirakami Y, Sakai H *et al.* (−)-Epigallocatechin gallate suppresses azoxymethane-induced colonic premalignant lesions in male C57BL/KsJ-*db/db* mice. *Cancer Prev Res* 2008; 1: 298–304.
20 Pretlow TP, O'Riordan MA, Somich GA, Amini SB, Pretlow TG. Aberrant crypts correlate with tumor incidence in F344 rats treated with azoxymethane and phytate. *Carcinogenesis* 1992; 13: 1509–12.
21 Bird RP. Role of aberrant crypt foci in understanding the pathogenesis of colon cancer. *Cancer Lett* 1995; 93: 55–71.
22 Xiao H, Hao X, Simi B *et al.* Green tea polyphenols inhibit colorectal aberrant crypt foci (ACF) formation and prevent oncogenic changes in dysplastic ACF in azoxymethane-treated F344 rats. *Carcinogenesis* 2008; 29: 113–9.
23 Jeong YI, Jung ID, Lee JS, Lee CM, Lee JD, Park YM. (−)-Epigallocatechin gallate suppresses indoleamine 2,3-dioxygenase expression in murine dendritic cells: evidences for the COX-2 and STAT1 as potential targets. *Biochem Biophys Res Commun* 2007; 354: 1004–9.
24 Cheng CW, Shieh PC, Lin YC *et al.* Indoleamine 2,3-dioxygenase, an immunomodulatory protein, is suppressed by (−)-epigallocatechin-3-gallate via blocking of gamma-interferon-induced JAK-PKC-delta-STAT1 signaling in human oral cancer cells. *J Agric Food Chem* 2010; 58: 887–94.
25 Yamada Y, Yoshimi N, Hirose Y *et al.* Sequential analysis of morphological and biological properties of beta-catenin-accumulated crypts, provable premalignant lesions independent of aberrant crypt foci in rat colon carcinogenesis. *Cancer Res* 2001; 61: 1874–8.
26 Shimizu M, Sakai H, Shirakami Y *et al.* Preventive effects of (−)-epigallocatechin gallate on diethylnitrosamine-induced liver tumorigenesis in obese and diabetic C57BL/KsJ-*db/db* mice. *Cancer Prev Res* 2011; 4: 396–403.
27 Wang ZY, Agarwal R, Bickers DR, Mukhtar H. Protection against ultraviolet B radiation-induced photocarcinogenesis in hairless mice by green tea polyphenols. *Carcinogenesis* 1991; 12: 1527–30.
28 Moolenbeek C, Ruitenberg EJ. The "Swiss roll": a simple technique for histological studies of the rodent intestine. *Lab Anim* 1981; 15: 57–9.
29 Bird RP. Observation and quantification of aberrant crypts in the murine colon treated with a colon carcinogen: preliminary findings. *Cancer Lett* 1987; 37: 147–51.
30 Suzuki R, Kohno H, Yasui Y *et al.* Diet supplemented with citrus unshiu segment membrane suppresses chemically induced colonic preneoplastic lesions and fatty liver in male *db/db* mice. *Int J Cancer* 2007; 120: 252–8.
31 Sakai H, Yamada Y, Shimizu M, Saito K, Moriwaki H, Hara A. Genetic ablation of Tnfalpha demonstrates no detectable suppressive effect on inflammation-related mouse colon tumorigenesis. *Chem Biol Interact* 2010; 184: 423–30.
32 Hoshi M, Saito K, Hara A *et al.* The absence of IDO upregulates type I IFN production, resulting in suppression of viral replication in the retrovirus-infected mouse. *J Immunol* 2010; 185: 3305–12.
33 Suzuki Y, Suda T, Furuhashi K *et al.* Increased serum kynurenine/tryptophan ratio correlates with disease progression in lung cancer. *Lung Cancer* 2010; 67: 361–5.
34 Fujigaki S, Saito K, Sekikawa K *et al.* Lipopolysaccharide induction of indoleamine 2,3-dioxygenase is mediated dominantly by an IFN-gamma-independent mechanism. *Eur J Immunol* 2001; 31: 2313–8.
35 Fujigaki S, Saito K, Takemura M *et al.* The L-Tryptophan–L-kynurenine pathway metabolism accelerated by *Toxoplasma gondii* infection is abolished in gamma interferon-gene-deficient mice: cross-regulation between inducible nitric oxide synthase and indoleamine-2,3-dioxygenase. *Infect Immun* 2002; 70: 779–86.
36 Shimizu M, Shirakami Y, Iwasa J *et al.* Supplementation with branched-chain amino acids inhibits azoxymethane-induced colonic preneoplastic lesions in male C57BL/KsJ-*db/db* mice. *Clin Cancer Res* 2009; 15: 3068–75.
37 Yasuda Y, Shimizu M, Shirakami Y *et al.* Pitavastatin inhibits azoxymethane-induced colonic preneoplastic lesions in C57BL/KsJ-*db/db* obese mice. *Cancer Sci* 2010; 101: 1701–7.
38 Katz JB, Muller AJ, Prendergast GC. Indoleamine 2,3-dioxygenase in T-cell tolerance and tumoral immune escape. *Immunol Rev* 2008; 222: 206–21.
39 Dolusic E, Larrieu P, Moineaux L *et al.* Tryptophan 2,3-dioxygenase (TDO) inhibitors. 3-(2-(pyridyl)ethenyl)indoles as potential anticancer immunomodulators. *J Med Chem* 2011; 54: 5320–34.
40 Carlin JM, Borden EC, Sondel PM, Byrne GI. Interferon-induced indoleamine 2,3-dioxygenase activity in human mononuclear phagocytes. *J Leukoc Biol* 1989; 45: 29–34.
41 Takikawa O, Tagawa Y, Iwakura Y, Yoshida R, Truscott RJ. Interferon-gamma-dependent/independent expression of indoleamine 2,3-dioxygenase. Studies with interferon-gamma-knockout mice. *Adv Exp Med Biol* 1999; 467: 553–7.

© 2012 Japanese Cancer Association

42 von Bergwelt-Baildon MS, Popov A, Saric T *et al.* CD25 and indoleamine 2,3-dioxygenase are up-regulated by prostaglandin E_2 and expressed by tumor-associated dendritic cells *in vivo*: additional mechanisms of T-cell inhibition. *Blood* 2006; 108: 228–37.
43 Basu GD, Tinder TL, Bradley JM *et al.* Cyclooxygenase-2 inhibitor enhances the efficacy of a breast cancer vaccine: role of IDO. *J Immunol* 2006; 177: 2391–402.
44 Shimizu K, Kinouchi Shimizu N, Hakamata W, Unno K, Asai T, Oku N. Preventive effect of green tea catechins on experimental tumor metastasis in senescence-accelerated mice. *Biol Pharm Bull* 2010; 33: 117–21.
45 Chung KT, Gadupudi GS. Possible roles of excess tryptophan metabolites in cancer. *Environ Mol Mutagen* 2011; 52: 81–104.
46 Koblish HK, Hansbury MJ, Bowman KJ *et al.* Hydroxyamidine inhibitors of indoleamine-2,3-dioxygenase potently suppress systemic tryptophan catabolism and the growth of IDO-expressing tumors. *Mol Cancer Ther* 2010; 9: 489–98.
47 Munn DH, Sharma MD, Mellor AL. Ligation of B7-1/B7-2 by human $CD4^+$ T cells triggers indoleamine 2,3-dioxygenase activity in dendritic cells. *J Immunol* 2004; 172: 4100–10.
48 Raju J. Azoxymethane-induced rat aberrant crypt foci: relevance in studying chemoprevention of colon cancer. *World J Gastroenterol* 2008; 14: 6632–5.
49 Gupta AK, Pretlow TP, Schoen RE. Aberrant crypt foci: what we know and what we need to know. *Clin Gastroenterol Hepatol* 2007; 5: 526–33.
50 Mori H, Hata K, Yamada Y, Kuno T, Hara A. Significance and role of early-lesions in experimental colorectal carcinogenesis. *Chem Biol Interact* 2005; 155: 1–9.
51 Yasui Y, Suzuki R, Kohno H *et al.* 9*trans*,11*trans* conjugated linoleic acid inhibits the development of azoxymethane-induced colonic aberrant crypt foci in rats. *Nutr Cancer* 2007; 59: 82–91.
52 Eleftheriadis T, Antoniadi G, Liakopoulos V, Stefanidis I, Galaktidou G. Plasma indoleamine 2,3-dioxygenase concentration is increased in hemodialysis patients and may contribute to the pathogenesis of coronary heart disease. *Renal Fail* 2012; 34: 68–72.

doi: 10.1111/j.1349-7006.2012.02237.x
© 2012 Japanese Cancer Association

J Cancer Res Clin Oncol (2013) 139:845–852
DOI 10.1007/s00432-013-1389-1

ORIGINAL PAPER

Hepatocellular carcinoma patients with increased oxidative stress levels are prone to recurrence after curative treatment: a prospective case series study using the d-ROM test

Yusuke Suzuki · Kenji Imai · Koji Takai · Tatsunori Hanai · Hideki Hayashi · Takafumi Naiki · Yoichi Nishigaki · Eiichi Tomita · Masahito Shimizu · Hisataka Moriwaki

Received: 31 October 2012 / Accepted: 30 January 2013 / Published online: 15 February 2013
© Springer-Verlag Berlin Heidelberg 2013

Abstract
Purpose Oxidative stress plays an important role in liver carcinogenesis. To determine the impact of oxidative stress on the recurrence of stage I/II hepatocellular carcinoma (HCC) after curative treatment, we conducted a prospective case series analysis.
Methods This study included 45 consecutive patients with stage I/II HCC, who underwent curative treatment by surgical resection or radiofrequency ablation at Gifu Municipal Hospital from 2006 to 2007. In these 45 cases, recurrence-free survival was estimated using the Kaplan–Meier method. The factors contributing to HCC recurrence, including the serum levels of derivatives of reactive oxygen metabolites (d-ROM) as an index of oxidative stress, were subjected to univariate and multivariate analyses using the Cox proportional hazards model.
Results The serum levels of d-ROM ($P = 0.0231$), α-fetoprotein (AFP, $P = 0.0274$), and fasting plasma glucose ($P = 0.0400$) were significantly associated with HCC recurrence in the univariate analysis. Multivariate analysis showed that the serum levels of d-ROM (hazard ratio [HR] 1.0038, 95 % confidence interval [CI] 1.0002–1.0071, $P = 0.0392$) and AFP (HR 1.0002, 95 % CI 1.0000–1.0003, $P = 0.0316$) were independent predictors of HCC recurrence. Kaplan–Meier analysis showed that recurrence-free survival was low in patients with high serum d-ROM (≥570 Carr U, $P = 0.0036$) and serum AFP (≥40 ng/dL, $P = 0.0185$) levels.
Conclusions The serum levels of d-ROM and AFP can be used for screening patients with a high risk for HCC recurrence. Patients who show increased levels of these factors require careful surveillance.

Keywords Hepatocellular carcinoma · Oxidative stress · d-ROM · Carcinogenesis

Introduction

Hepatocellular carcinoma (HCC) is one of the most common malignancies worldwide, accounting for 750,000 annual cases; approximately the same number of people (700,000) die from this malignancy each year (Jemal et al. 2011). HCC development is frequently associated with chronic inflammation and subsequent cirrhosis of the liver induced by persistent infection with hepatitis B virus (HBV) or hepatitis C virus (HCV) (El-Serag 2002). Alcohol consumption, obesity, and related metabolic disorders such as diabetes mellitus are also involved in liver carcinogenesis (El-Serag 2002). The prognosis of patients with HCC is poor because the incidence of recurrence in patients with underlying cirrhosis is very high (Toyama et al. 2008). Therefore, careful surveillance of high-risk groups for HCC and early detection before progression to an advanced stage are important to improve the prognosis of this malignancy. It is therefore a task of pressing urgency to identify useful risk factors for HCC development or recurrence. Male gender, the presence of cirrhosis,

Electronic supplementary material The online version of this article (doi:10.1007/s00432-013-1389-1) contains supplementary material, which is available to authorized users.

Y. Suzuki · H. Hayashi · Y. Nishigaki · E. Tomita
Department of Gastroenterology,
Gifu Municipal Hospital, Gifu, Japan

K. Imai · K. Takai · T. Hanai · T. Naiki · M. Shimizu (✉) · H. Moriwaki
Department of Medicine, Gifu University Graduate School of Medicine, 1-1 Yanagido, Gifu 501-1194, Japan
e-mail: shimim-gif@umin.ac.jp

high α-fetoprotein (AFP), large tumor foci, multiplicity of tumors, pathologically high-grade atypia of tumor cells, and the presence of portal venous invasion of tumors are thought to increase the risk for HCC recurrence (Ikeda et al. 1993; Koike et al. 2000). The increased Homeostatic Model Assessment of Insulin Resistance (HOMA-IR) value, which reflects insulin resistance, and high levels of serum leptin, one of the adipokines associated with obesity, are also independent risk factors for HCC recurrence (Imai et al. 2010; Watanabe et al. 2011).

Increased evidence indicates that continuous oxidative stress, which results from the imbalance between the production of reactive oxygen species (ROS) and the antioxidant defense mechanisms, plays a critical role in the development of various human malignancies, including HCC (Sasaki 2006; Valko et al. 2007; Sakurai et al. 2008). As a major site of metabolism, the liver displays high levels of ROS resulting in increased oxidative stress. Oxidative stress is known to induce DNA damage, and accumulation of such genetic damage can eventually contribute to liver carcinogenesis (Sasaki 2006; Valko et al. 2007; Sakurai et al. 2008). HCV infection is associated with elevated levels of ROS and decreased antioxidant levels in patients (Seronello et al. 2007). Oxidative stress has been associated with the development of steatosis and liver tumors in HCV core transgenic mice (Moriya et al. 2001). In addition, increased levels of ROS is also involved in migration, invasion, and metastasis of HCC cells (Hu et al. 2011; Chung et al. 2012). These findings suggest that oxidative stress biomarkers might potentially be useful for predicting the development and recurrence of HCC in patients with chronic liver disease. Clinical studies using liver specimens obtained by biopsy or surgery have shown the predictive power of oxidative stress biomarkers on HCC development (Chuma et al. 2008; Tanaka et al. 2011). However, serum oxidative stress biomarkers predictive for recurrence after curative treatment for HCC have not been investigated.

Quantification of derivatives of reactive oxygen metabolites (d-ROM) is a simple method for detecting hydroperoxide levels (Trotti et al. 2002), and clinical trials have shown that the d-ROM test is useful for evaluating oxidative stress (Trotti et al. 2002; Hirose et al. 2009; Sugiura et al. 2011). In this study, we measured the serum d-ROM level in patients with HCC and designed a prospective case series analysis to examine the recurrence-free survival in consecutive patients with stage I/II HCC who received curative treatment by surgical resection or radiofrequency ablation (RFA), stratified according to the serum d-ROM level. Thus, the aim of the present study was to determine whether the d-ROM test is useful as a marker of oxidative stress for evaluating HCC recurrence risk in the clinical setting.

Patients and methods

Patients

We evaluated 45 consecutive primary HCC patients in Gifu Municipal Hospital from 2006 to 2007, all of whom met the following criteria: tumor stage classified as I or II and surgical resection or RFA as the initial treatment. Tumor stage was defined according to the staging system of the Liver Cancer Study Group of Japan (2010). HCC nodules were detected using imaging modalities including dynamic computed tomography (CT), dynamic magnetic resonance imaging (MRI), and abdominal arteriography. HCC was diagnosed from a typical hypervascular tumor stain on angiography and typical dynamic study findings of enhanced staining in the early phase and attenuation in the delayed phase.

Treatment, follow-up, and determination of recurrence

One patient was treated with surgical resection, 41 with RFA, and 3 with RFA after transarterial chemoembolization. The selection criteria for the initial treatments were determined according to the Clinical Practice Guidelines for HCC by the Japan Society of Hepatology (Clinical Practice Guidelines for Hepatocellular Carcinoma—The Japan Society of Hepatology 2009 update 2010). The response to treatment was defined as complete response when dynamic CT or MRI showed complete disappearance of the HCC imaging characteristics in all target lesions, according to the Response Evaluation Criteria in Cancer of the Liver (Kudo et al. 2010).

Patients were thereafter followed up on an outpatient basis by assessing the levels of serum tumor markers such as AFP and proteins induced by vitamin K absence or antagonist-II (PIVKA-II) every month and by using imaging modalities such as abdominal ultrasonography, dynamic CT scanning, or dynamic MRI every 3 months. Recurrent HCC was defined as the appearance of distant lesions to exclude local recurrence. Consequently, recurrent HCC was further classified into multicentric occurrence or intrahepatic metastasis by CT images according to the definition by the Liver Cancer Study Group of Japan (Liver Cancer Study Group of Japan 2010). The follow-up period was defined as the interval from the date of initial treatment until the date of diagnosis of recurrence or until March 2012 if HCC did not recur.

Oxidative stress assay

Before curative treatment, oxidative stress was assessed by measuring the serum hydroperoxide concentration according to the d-ROM test (Diacron srl, Grosseto, Italy) by

Table 1 Baseline demographic and clinical characteristics

Variables	$n = 45$
Sex (male/female)	30/15
Age (years)	72 [50–82]
BMI (kg/m^2)	22.8 [15.6–33.5]
Etiology (B/C/B + C/other)	3/40/1/1
Follow-up period (days)	1,707 [305–2,231]
d-ROM (Carr U)	496 [295–869]
Child-Pugh classification (A/B/C)	33/12/0
ALB (g/dL)	3.5 [2.6–4.5]
ALT (IU/L)	51 [12–100]
T-Bil (mg/dL)	1.0 [0.5–3.7]
PLT ($\times 10^4/\mu$L)	9.8 [3.6–19.5]
PT (%)	71 [50–100]
FPG (mg/dL)	100 [41–224]
HbA_{1c} (%)[a]	5.7 [4.0–9.8]
AFP (ng/dL)	32.5 [1.7–16,931]
PIVKA-II (mAU/mL)	23.0 [5–1,860]
Stage (I/II)	21/24
Tumor size (cm)	1.7 [1.0–5.3]
Tumor number (1/2/3/4)	36/6/1/2
Portal vein invasion (yes/no)	0/45
Initial treatment for HCC (resection/RFA/TACE + RFA)	1/41/3

Values are presented as median [range]. *BMI* body mass index, *d-ROM* derivatives of reactive oxygen metabolites, *ALB* albumin, *ALT* alanine aminotransferase, *T-Bil* total bilirubin, *PLT* platelet count, *PT* prothrombin time, *FPG* fasting plasma glucose, HbA_{1c} hemoglobin A1c, *AFP* α-fetoprotein, *PIVKA-II* protein induced by vitamin K absence or antagonists-II, *RFA* radiofrequency ablation, *TACE* transarterial chemoembolization

[a] HbA_{1c} is presented in National Glycohemoglobin Standardization Program units

using a free radical elective evaluator, FREE (Diacron srl), as described previously (Trotti et al. 2002; Hirose et al. 2009; Sugiura et al. 2011).

Statistical analysis

Recurrence-free survival was estimated using the Kaplan–Meier method, and differences between curves were evaluated using the logrank test. Baseline characteristics were compared using the Student's t test for continuous variables or the χ^2 test for categorical variables. Eleven possible predictors for HCC recurrence after initial curative treatment were selected as follows: sex, age, body mass index (BMI), Child-Pugh classification, serum albumin level, platelet count, fasting plasma glucose (FPG), serum AFP level, serum PIVKA-II level, tumor stage, and the serum d-ROM level. Parameters determined to be significant according to univariate analysis were then subjected to multivariate analysis using the Cox proportional hazards model. Receiver operating characteristic (ROC) analysis was used to identify the cut-off values for d-ROM and AFP that would best predict HCC recurrence. Statistical significance was defined as $P \setminus 0.05$.

Results

Baseline characteristics and laboratory data of patients

The baseline characteristics and laboratory data of the 45 patients (30 men and 15 women, median age: 72 years) are shown in Table 1. The median follow-up period was 1,707 days (range 305–2,231 days). Thirty-three patients were classified as Child-Pugh class A, 12 patients as class B, and none as class C. The median d-ROM level of all the patients with HCC was 496 Carr U (range 295–869 Carr U).

Possible risk factors for HCC recurrence

In all 45 curative cases of stage I/II HCC, 41 patients experienced recurrence in the liver and 2 patients exhibited distant metastasis; 1 in the lung and the other in the bone. The 1-year, 3-year, and 5-year recurrence-free survival rates in the 45 patients were 60, 29, and 7 %, respectively (Fig. 1a). Among 41 cases that caused intrahepatic recurrence of HCC, 36 cases were diagnosed as multicentric occurrence and the others (5 cases) were as intrahepatic metastasis, respectively.

At first, we analyzed possible risk factors for total recurrence including both multicentric occurrence and intrahepatic metastasis by the Cox proportional hazards model using the 11 variables listed in Table 2. The serum d-ROM level (hazard ratio [HR] 1.0036, 95 % confidence interval [CI] 1.0005–1.0070, $P = 0.0231$), serum AFP level (HR 1.0001, 95 % CI 1.0000–1.0002, $P = 0.0274$), and FPG (HR 1.0008, 95 % CI 1.0004–1.0157, $P = 0.0400$) were significantly associated with HCC recurrence in univariate analysis. Among these variables, multivariate analysis indicated that serum levels of d-ROM (HR 1.0038, 95 % CI 1.0002–1.0071, $P = 0.0392$) and AFP (HR 1.0002, 95 % CI 1.0000–1.0003, $P = 0.0316$) were independent predictors of HCC recurrence (Table 3).

The cut-off values of d-ROM (570 Carr U) and AFP (40 ng/dL) for the prediction of HCC recurrence were determined by ROC analysis. Kaplan–Meier analysis showed that recurrence-free survival was lower in patients with high serum d-ROM levels (≥570 Carr U, $P = 0.0036$) (Fig. 1b) and in those with high serum AFP levels (≥40 ng/dL, $P = 0.0185$) (Fig. 1c). Table 4 shows the baseline characteristics and laboratory data of patients

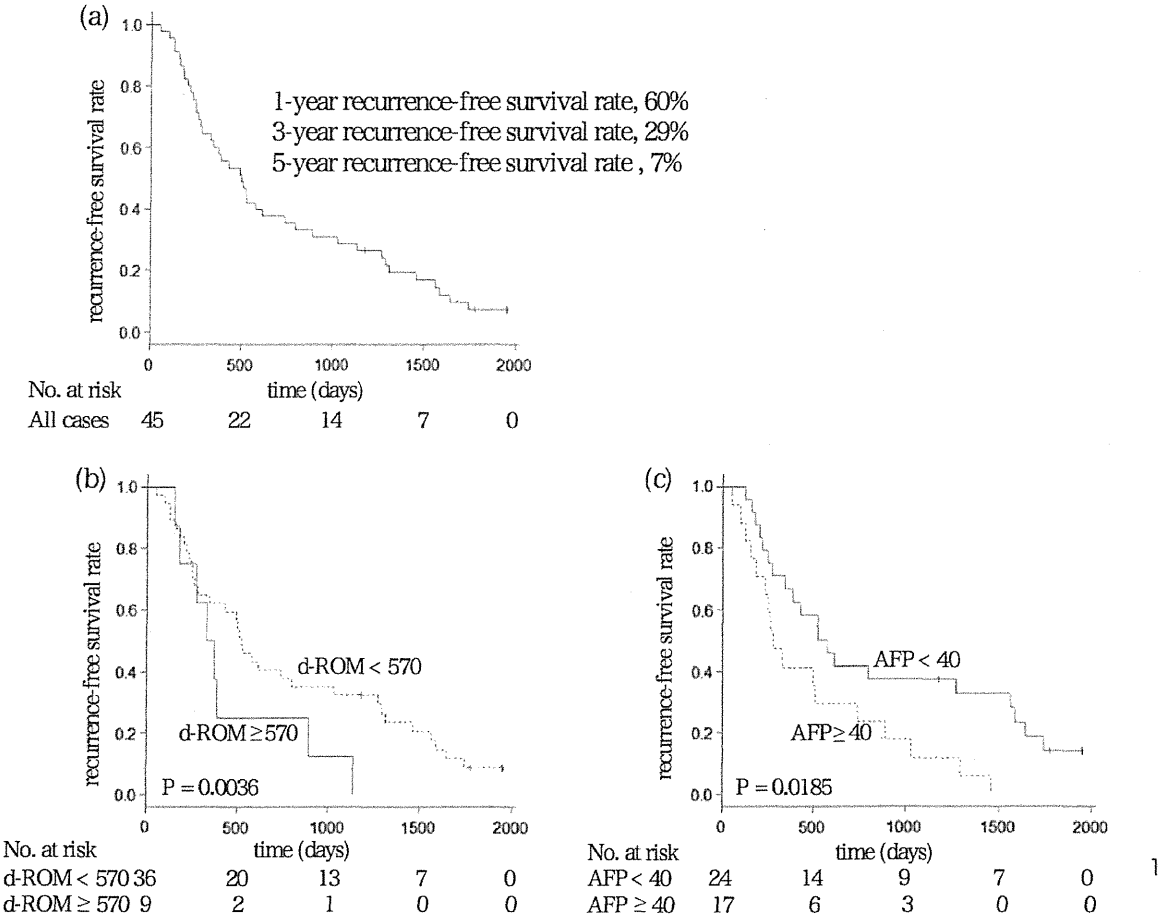

Fig. 1 Kaplan–Meier curves for recurrence-free survival in (**a**) all patients and in subgroups of patients, divided according to (**b**) d-ROM levels or (**c**) serum AFP levels

Table 2 Univariate analyses of possible risk factors for hepatocellular carcinoma recurrence according to a Cox proportional hazards model

Variable	HR	95 % CI		*P* value
		Lower limit	Upper limit	
Sex (male vs. female)	0.9142	0.4810	1.8307	0.7917
Age (years)	1.0086	0.9714	1.0473	0.6522
BMI (kg/m^2)	0.9878	0.9082	1.0696	0.7695
Child-Pugh classification (B vs. A)	0.9707	0.4643	1.8843	0.9329
ALB (g/dL)	0.9496	0.4600	1.9744	0.8893
PLT ($\times 10^4$/mL)	0.9817	0.9031	1.0613	0.6507
FPG (mg/dL)	1.0008	1.0004	1.0157	0.0400
AFP (ng/dL)	1.0001	1.0000	1.0002	0.0274
PIVKA-II (mAU/mL)	1.0005	0.9996	1.0012	0.2149
Stage (II vs. I)	1.1968	0.6468	2.2348	0.5664
d-ROM (Carr U)	1.0036	1.0005	1.0070	0.0231

CI confidence interval, *HR* hazard radio, *BMI* body mass index, *ALB* albumin, *PLT* platelets, *FPG* fasting plasma glucose, *AFP* α-fetoprotein, *PIVKA-II* protein induced by vitamin K absence or antagonists-II, *d-ROM* derivatives of reactive oxygen metabolites

divided on the basis of the serum d-ROM concentration (\ 570 Carr U and ≥ 570 Carr U). No significant differences were noted between the 2 subgroups.

The serum d-ROM levels were not significantly correlated with any clinical factors associated with hepatic functional reserve (serum total bilirubin, serum albumin,

Table 3 Multivariate analyses of possible risk factors for hepatocellular carcinoma recurrence according to a Cox proportional hazards model

Variable	HR	95 % CI		*P* value
		Lower limit	Upper limit	
FPG (mg/dL)	1.0004	0.9961	1.0126	0.2699
AFP (ng/dL)	1.0002	1.0000	1.0003	0.0316
d-ROM (Carr U)	1.0038	1.0002	1.0071	0.0392

CI confidence interval, *HR* hazard radio, *FPG* fasting plasma glucose, *AFP* α-fetoprotein, *d-ROM* derivatives of reactive oxygen metabolites

serum alanine aminotransferase, prothrombin time, and platelet count) and HCC (tumor size, AFP, and PIVKA-II) (Table 5). In addition, the d-ROM levels did not show significant relationships between the clinical factors for diabetes, including FPG, HbA_{1c}, fasting immunoreactive insulin, and HOMA-IR (Table 5), although several studies have reported that oxidative stress increases with the presence of diabetes and that the d-ROM level is correlated with diabetic factors (Vassalle et al. 2008; Hirose et al. 2009; Sugiura et al. 2011). Further, no significant differences in the median values of d-ROM were noted between (1) the Child-Pugh class A group (496 Carr U, range 295–869 Carr U) and the Child-Pugh class B group (500 Carr U, range 314–589 Carr U) and (2) the stage I group (516 Carr U, range 295–858 Carr U) and the stage II group (500 Carr U, range 314–869 Carr U), suggesting that d-ROM values were not associated with hepatic functional reserve, tumor factors, or the presence of diabetes in this study. These findings indicate that an increased d-ROM value was independently related to the recurrence of HCC.

A separate analysis of 36 multicentric occurrence cases showed an inverse correlation between the serum d-ROM levels and the recurrence-free period, but the significance was marginal ($P = 0.0512$) due to the small number of patients (data not shown). In addition, intrahepatic metastasis cases ($N = 5$) showed a higher d-ROM levels (median 614 Carr U, range 496–869 Carr U) than non-recurrent cases ($N = 4$, median 474 Carr U, range: 461–509 Carr U) ($P = 0.112$).

Discussion

Increasing evidence suggests that oxidative stress plays a critical role in liver carcinogenesis (Sasaki 2006; Sakurai et al. 2008). Elevation of ROS can cause oxidative damage to important cellular macromolecules such as DNA, proteins, and lipids (Valko et al. 2007). Excessive ROS also disrupts the cell signaling pathways that are involved in cell growth and survival, leading further to the advanced stage of carcinogenesis, and cancer promotion and progression (Dreher and Junod 1996; Carmeliet 2000).

Table 4 Baseline demographic and clinical characteristics of patients classified according to the d-ROM level

	d-ROMs \ 570 ($n = 36$)	d-ROMs ≥ 570 ($n = 9$)	*P* value
Sex (male/female)	24/12	6/3	1.0000
Age (years)	72 [50–82]	69 [58–76]	0.5325
BMI	22.5 [15.6–33.5]	23.0 [20.1–27.0]	0.7965
Etiology (B/C/B + C/other)	3/31/1/1	0/9/0/0	0.4968
Follow-up period (days)	1,712 [458–2,231]	1,643 [305–2,146]	0.2350
Child-Pugh classification (A/B)	26/10	7/2	0.7323
ALB (g/dL)	3.5 [2.6–4.5]	3.5 [3.0–4.4]	0.9312
ALT (IU/L)	48 [12–100]	53 [22–73]	0.5621
T-Bil (mg/dL)	1.0 [0.5–3.7]	1.0 [0.6–1.5]	0.8532
PLT ($\times 10^4/\mu L$)	10.4 [3.8–19.5]	6.6 [3.6–18.8]	0.0843
PT (%)	70 [50–100]	77 [59–90]	0.2293
FPG (mg/dL)	99 [41–224]	104 [83–140]	0.6272
HbA_{1c} (%)[a]	5.7 [4.0–9.8]	5.3 [4.8–7.0]	0.6447
AFP (ng/dL)	31 [1.7–16,931]	33 [16.7–210]	0.5130
PIVKA-II (mAU/mL)	19.5 [5–1,540]	57.0 [7–1,860]	0.2822
Stage (I/II)	17/19	4/5	0.8811
Initial treatment for HCC (resection/RFA/TACE + RFA)	1/32/3	0/9/0	0.3905

Values are presented as median [range]. *BMI* body mass index, *ALB* albumin, *ALT* alanine aminotransferase, *T-Bil* total bilirubin, *PLT* platelets, *PT* prothrombin time, *FPG* fasting plasma glucose, *HbA_{1c}* hemoglobin A1c, *AFP* α-fetoprotein, *PIVKA-II* protein induced by vitamin K absence or antagonists-II, *HCC* hepatocellular carcinoma

[a] HbA_{1c} is presented in National Glycohemoglobin Standardization Program units